AGU PUBLICATIONS

JGR

Journal of Geophysical Research: Solid Earth

RESEARCH ARTICLE
10.1002/2017JB014387

Key Points:
- We propose a mechanism to explain persistent hot crater lakes at volcanoes and investigate their controlling parameters
- Two patterns of change are seen in modeled hot crater lakes before eruptions and applied to field data
- Apparent volcanic unrest due to topographic effects can occur without increased subaqueous fumarolic activity

Correspondence to:
A. Terada,
terada@ksvo.titech.ac.jp

Citation:
Terada, A., and T. Hashimoto (2017), Variety and sustainability of volcanic lakes: Response to subaqueous thermal activity predicted by a numerical model, *J. Geophys. Res. Solid Earth*, *122*, 6108–6130, doi:10.1002/2017JB014387.

Received 1 MAY 2017
Accepted 21 JUL 2017
Accepted article online 24 JUL 2017
Published online 14 AUG 2017

Variety and sustainability of volcanic lakes: Response to subaqueous thermal activity predicted by a numerical model

Akihiko Terada[1] **and Takeshi Hashimoto**[2]

[1]Volcanic Fluid Research Center, School of Science, Tokyo Institute of Technology, Tokyo, Japan, [2]Institute of Seismology and Volcanology, Faculty of Science, Hokkaido University, Sapporo, Japan

Abstract We use a numerical model to investigate the factors that control the presence or absence of a hot crater lake at an active volcano. We find that given a suitable pair of parameters (e.g., the enthalpy of subaqueous fumaroles and the ratio of mass flux of the fluid input at the lake bottom to lake surface area), hot crater lakes can be sustained on relatively long timescales. Neither a high rate of precipitation nor an impermeable layer beneath the lake bottom are always necessary for long-term sustainability. The two controlling parameters affect various hydrological properties of crater lakes, including temperature, chemical concentrations, and temporal variations in water levels. In the case of low-temperature crater lakes, increases in flux and enthalpy, which are a common precursor to phreatic or phreatomagmatic eruptions, result in an increase in both temperature and water level. In contrast, a decrease in water level accompanied by a rise in temperature occurs at high-temperature lakes. Furthermore, our model suggests that crater geometry is a key control on water temperature. For lakes with a conical topography, a perturbation in the water level due to trivial nonvolcanic activity, such as low levels of precipitation, can cause persistent increases in water temperature and chemical concentrations, and a decrease in the water level, even though subaqueous fumarolic activity does not change. Such changes in hot crater lakes which are not caused by changes in volcanic activity resemble the volcanic unrest that precedes eruptions.

Plain Language Summary The existence of a volcanic crater lake can increase volcanic hazard. Volcanic explosions at crater lakes can be accompanied by tsunamis or base surges. In this study, we develop a numerical model to investigate the factors that control the presence or absence of a hot crater lake at an active volcano. Neither a high rate of precipitation nor an impermeable layer beneath the lake bottom is always necessary for long-term sustainability. Our model predicts two types of a hot crater lake: in the case of low-temperature crater lakes, increases in subaqueous fumarolic activity, which are a common precursor to eruptions, result in an increase in both temperature and water level. In contrast, boiling dry occurs at high-temperature lakes. Furthermore, our model predicts that crater geometry is a key control on water temperature. For lakes with a conical topography, a perturbation in the water level due to trivial nonvolcanic activity, such as low levels of precipitation, can cause persistent increases in water temperature and chemical concentrations. Such changes in hot crater lakes resemble the volcanic unrest that precedes eruptions, referred to as "apparent volcanic unrest."

1. Introduction

The existence of a volcanic crater lake can increase volcanic hazard. Phreatic and phreatomagmatic explosions at crater lakes can be accompanied by tsunamis or base surges after the collapse of an eruption column [*Morrissey et al.*, 2010]. These eruptions can cause devastating lahars owing to drainage of lake water or snowmelt [*Cronin et al.*, 1997; *Lecointre et al.*, 2004; *Schaefer et al.*, 2008], which can be the most dangerous hazard for people near the lake shore and inhabitants along any river that drains from the crater lake [*Mastin and Witter*, 2000].

Hot crater lakes at volcanoes act as condensers of heat, volatiles, and materials released from hydrothermal systems associated with magma bodies [*Brantley et al.*, 1993], so that measurements of water levels or crater-lake temperatures can be used to predict eruptions [*Brown et al.*, 1989]. Regular sampling of lake water at hot crater lakes has been used to monitor many volcanic systems, including Ruapehu [*Giggenbach and Glover*, 1975; *Hurst et al.*, 1991], Kusatsu-Shirane [*Ohba et al.*, 1994; *Ohba et al.*, 2008], and Poás [*Rowe et al.*, 1992; *Martinez et al.*, 2000; *Rouwet et al.*, 2016]. These results indicate that changes in the Mg and Cl

concentrations of lake water are useful when monitoring changes in subaqueous fumaroles; however, sampling lake water is difficult at some crater lakes, such as Aso volcano. *Barberi et al*. [1992] reported 19 cases in which water temperature and level of crater lake changed several weeks to a few days before eruptions. It is notable that increases in both water level and temperature were observed in most cases, but a decrease in water level accompanied by a temperature increase occurred in 2 of 19 cases [*Barberi et al*., 1992]. Changes in lake levels seem to be caused by changes in subaqueous fumaroles; however, the physical mechanisms that drive these changes are not yet well understood. To interpret changes in volcanic activity based on observations of hot crater lakes, it is necessary to understand the state of mass balance in the crater lakes.

There is some uncertainty regarding the factors that control whether a volcano has a hot crater lake. Until recently, it was believed that approximately 12% of 714 Holocene-age volcanoes contain volcanic lakes [*Rowe et al*., 1992; *Simkin and Siebert*, 1994; *Pasternack and Varekamp*, 1997]. However, data from 474 volcanic lakes were compiled in a database by *Rouwet et al*. [2014], indicating that there are more volcanic lakes on Earth than previously reported. The occurrence of an impermeable layer may explain the existence of volcanic lakes. Indeed, magnetotelluric surveys [*Kanda et al*., 2008] detected a layer of hydrothermal alteration at 100−200 m beneath the floor of Yudamari, a hot crater lake at Aso volcano, Japan [*Terada et al*., 2012; *Shinohara et al*., 2015], which may act as an impermeable layer. However, it is plausible that past volcanic explosions repeatedly destroyed the crater floor, including the underlying impermeable alteration layer, and replaced it with fresh eruption material. At the first crater of Nakadake, which contains Yudamari lake, phreatomagmatic and Strombolian eruptions have occurred over the past 1500 years [*Miyabuchi*, 2009], including a major sequence of Strombolian eruptions in 1989–1991 [*Ono et al*., 1995]. Despite these eruptions, the lake always reforms in a similar state once the volcano returns to quiescence. Similar cyclical changes at hot crater lakes are seen at Laguna Caliente crater lake at Poás volcano, Costa Rica [*Brown et al*., 1989]; Ruapehu Crater Lake, New Zealand [*Christenson*, 2000]; and Copahue crater lake, on the Chile–Argentina border [*Varekamp et al*., 2001; *Tamburello et al*., 2015; *Agusto et al*., 2016].

Observations of volcanic lakes have revealed a variety of significant features [*Rouwet et al*., 2014]. *Pasternack and Varekamp* [1997] proposed an empirical classification scheme for volcanic lakes on the basis of water temperature, the stability of the water level, and geochemical features including pH, TDS (total dissolved solids, g/L), and chemical composition. These works show that volcanic lakes can be classified according to simple schemes, suggesting that simple mechanisms control their characteristics. Hot crater lakes can be regarded as sensitive to the magmatic and/or hydrothermal systems beneath the craters [*Vandemeulebrouck et al*., 2005]; thus, the geophysical and geochemical characteristics of volcanic lakes may reflect a variety of underlying magmatic hydrothermal systems.

To understand these variety in volcanic lake behavior and characteristics, we develop a generic numerical model of a hot crater lake. This model is intentionally simple, in that it does not assume values of seepage output or precipitation input. In the model, lake sustainability is a function of four dimensionless parameters, which can explain the variety of observed features summarized by *Pasternack and Varekamp* [1997] and *Rouwet et al*. [2014]. Based on our model, we propose a mechanism to explain persistent hot crater lakes at volcanoes. In addition, we show that two patterns of change are seen in hot crater lakes preceding eruptions. Furthermore, our model predicts that apparent volcanic unrest due to topographic effects can occur without increased volcanic activity. These results are useful for monitoring subaqueous geothermal activity without geochemical data, such as Mg and Cl concentrations.

2. Numerical Model of a Hot Crater Lake

2.1. Aim

In the present model, we consider that a hot crater lake lasts for a long time in the case that mass equilibrium is attained in the lake system. In such a situation, the water level remains constant over time, which we herein call "lake-sustainable conditions." We assess the stability of a hot crater lake under lake-sustainable conditions with respect to perturbations in water level and temperature.

Fluid injected from the lake bottom, which has an enthalpy higher than that of lake water, is an important factor in controlling changes in lake level. Indeed, high-enthalpy fluids may have two conflicting effects on

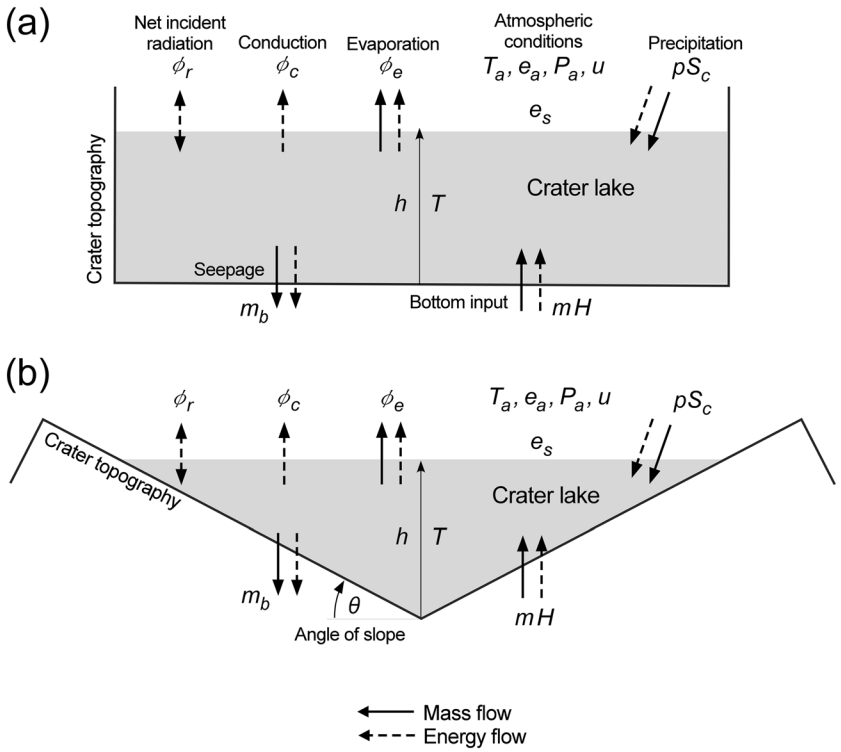

Figure 1. Schematic summary of the energy and mass inputs to and outputs from crater lakes. Parameters indicated are defined in Table 1. (a) Cylindrical and (b) conical topography are described in sections 3.1 and 3.2, respectively; abbreviations showing in Table 1 are common to both cases.

lake level: an increase in lake level due to an increase in fluid volume and a decrease in lake level because the high-enthalpy fluid causes an increase in water temperature, thereby enhancing evaporation. To assess the magnitude of lake level changes due to changes in the rate of supply of fluid at the lake bottom, it is necessary to simultaneously calculate trends in water temperature and evaporation mass over time.

Based on a numerical approach, *Pasternack and Varekamp* [1997] investigated lake water under various conditions. Their model suggested that lake temperatures are determined mainly by the magnitude of volcanic heat input relative to the surface area of the lake. In their analysis, they regarded the fluid injected from the lake bottom as a gas phase with a temperature expressed as a function of the gas mass flux; however, the supply of fluid in the liquid phase (e.g., groundwater inflow and recycling of seepage water) is known to be significant at some crater lakes [*Terada et al*., 2012]. The model employed by *Pasternack and Varekamp* [1997] also assumed no seepage outflow and a constant catchment area 1.5× the lake radius, which plays an important role in controlling the water level. In the present model, the mass and enthalpy of the fluid injected from the lake bottom, seepage outflow, and precipitation inflow are variable, in order to quantify their effects on water level.

2.2. Basic Assumptions

We simplify the system at a hot crater lake as depicted in Figure 1a. An essential assumption of this study is that fumaroles and/or hot-water fountains exist on the crater floor. These vents are covered by lake water, meaning that all mass and energy injected from the lake bottom are absorbed by the lake water. For simplicity, it is assumed that the lake water is well mixed; thus, the water temperature is assumed to be homogeneous. The temperature of the lake surface is one of the important factors that control the mass and energy balances of the lake system. The distribution of water temperatures should be examined if this model is to be applied to a real volcanic lake.

Lake water is supplied by fluid injection at the lake bottom and by precipitation inflow and is lost by evaporation from the lake surface and seepage through the lake bottom. Fluid injected from the lake bottom is a mixture of hot thermal water including two phase fluids, recycled seepage water, and underground water. Thermal

Table 1. Definitions of Abbreviations

Abbreviation	Definition
h	Lake depth, m
S	Lake surface area, m^2
S_c	Effective catchment area, m^2
V	Lake volume, m^3
T	Temperature of lake water, °C
H	Specific enthalpy of the fluid injected from the lake bottom, J kg^{-1}
m	Mass flux of fluid injected from the lake bottom, kg s^{-1}
m_b	Flux of seepage water through the lake bottom, kg s^{-1}
T_a	Air temperature of lake water, °C
e_a	Vapor pressure at 2 m above the lake surface, Pa
u	Wind velocity at 2 m above the lake surface, m s^{-1}
P_a	Air pressure, Pa
p	Precipitation rate, kg $m^{-2}s^{-1}$
Φ	Total heat flux from the lake surface, W m^{-2}
ϕ_e	Evaporation heat flux from the lake surface, W m^{-2}
ϕ_c	Conduction heat flux from the lake surface, W m^{-2}
ϕ_r	Net radiation heat flux from the lake surface, W m^{-2}
ρ	Density of lake water, kg m^{-3}
ρ	Density of lake water, kg m^{-3}
L	Latent heat of water at 50°C, 2.38×10^6 J kg^{-1}
i	Empirical constant for seepage rate
f	Empirical constant for catchment area
k	Parameter (one for cylindrical and one third for conical topography)
μ	Mass ratio of bottom input to evaporative loss
ε	Ratio of enthalpy of the bottom input to that of lake water
λ	Mass ratio of bottom input to seepage
γ	Mass ratio of bottom input to inflow by precipitation

energy is added to the lake in the form of fluid supply from the lake bottom and precipitation, as well as solar and atmospheric radiation, while it is lost by evaporative, conductive, and radiative heat transfer from the lake surface to the atmosphere and by seepage through the lake bottom. Conductive heat flow through the crater bottom and wall is ignored. This study considers a closed lake with no surface runoff outlets.

In this model, fluid injection from subaqueous fumaroles does not depend on seepage through the lake bottom. However, a hot crater lake and an underlying hydrothermal system can interact with one another [*Vandemeulebrouck et al.*, 2005]. In such a situation, an increase in the pressure of the hydrothermal system is likely caused by an increase in the water level. As a result, the fluid injection rate can be altered by changes in the liquid/vapor ratio and the temperature of the hydrothermal system. Thus, it is possible that fluid injection interacts with seepage. Quantitative evaluations of such interaction are complex, so that we do not discuss the underlying hydrothermal system, and we focus in this paper on phenomena that are caused by interactions between the atmosphere and crater lake through the lake surface.

2.3. Formulation

We simplify the numerical model of *Terada et al.* [2012] used to describe the above mentioned system, then apply it to assess the sustainability of hot crater lakes. The fluid injected from the lake bottom comprises vapor, hot water of volcanic origin, groundwater, and recycled seepage water from the lake. The total mass flux of fluid injected from the lake bottom is denoted m (kg s^{-1}). We define H (J kg^{-1}), the bottom input enthalpy per unit mass, as the average enthalpy among the fluids injected through the lake bottom.

Using V (m^3), the volume of lake water as a function of lake level h (m) and bulk water temperature T (°C), the equations of conservation of mass and energy for the lake water are respectively as follows:

$$\rho \frac{dV(h)}{dt} = m - \frac{\varphi_e S}{L} - m_b + pS_c \tag{1}$$

$$\rho C_{pw} \frac{d}{dt}[TV(h)] = Hm - \Phi S - m_b C_{pw} T + pS_c C_{pw} T_a, \tag{2}$$

where ρ (kg m^{-3}) is the mean density of the lake, S (m^2) is the lake surface area, L (J kg^{-1}) is the latent heat of the lake water, C_{pw} (J kg^{-1} K^{-1}) is the specific heat of the lake water (Table 1), and φ_e (J s^{-1} m^{-2}) is the evaporative heat flux (see Appendix).

The second term on the right-hand side of equation (1) represents the evaporative mass flux from the lake surface. The second term on the right-hand side of equation (2), Φ (J s^{-1} m^{-2}), is the heat flux from the lake surface, which is the sum of the heat fluxes due to evaporation φ_e, conduction φ_c, and radiation φ_r (J s^{-1} m^{-2}).

The third term on the right-hand side of equations (1) and (2), m_b (kg m^{-1}), is the seepage flux. Generally, seepage occurs through the crater bottom and crater wall. The seepage flux depends on the permeability

of the surrounding rocks and the pressure gradient, which are case-by-case parameters. To outline the effects on seepage to the lake system, we assume that seepage occurs through the lake bottom following Darcy's law. Thus, we assume that seepage flux is approximately given by

$$m_b = i\,\rho h S, \tag{3}$$

where i (s^{-1}) is an empirical constant.

In the last term in equations (1) and (2), p is precipitation (kg m^{-2} s^{-1}) and S_c (m^2) is the effective catchment area, which is expressed in terms of the characteristic surface area S_0 (m^2), as follows:

$$S_c = fS_0, \tag{4}$$

where f is an empirical constant.

Generally, the mass flux m and enthalpy H of the fluid injected from the lake bottom are not directly observable. To quantify them, we draw upon prior mass and energy balance studies [e.g., *Rowe et al*., 1992; *Brantley et al*., 1993; *Ohba et al*., 1994; *Rouwet et al*., 2004: *Fournier et al*., 2009; *Rouwet and Tassi*, 2011; *Terada et al*., 2012: *Rouwet et al*., 2016]. The seepage flux, m_b, is difficult to estimate for each case. Using the empirical relationship between seepage flux and equivalent lake volume [*Terada et al*., 2012, Figure 6], the constant i can be obtained. In *Terada et al*. [2012, Figure 6], the seepage flux of Laguna Caliente crater lake of Poás volcano is exceptionally large, around 450 kg s^{-1} [*Rowe et al*., 1992]; however, *Todesco et al*. [2015] estimate the seepage flux to be $1-10$ kg s^{-1}, which agrees with the empirical relationship.

Assuming that no changes in other parameters occur during these short intervals, an effective catchment area, S_c, can be empirically evaluated by measuring changes in lake volume before and after rainfall.

2.4. Numerical Analysis of Simple Crater Geometries Under Constant, Moderate Atmospheric Conditions

Here we compute temporal variations in lake level and temperature with the aim of determining the influence of parameters such as volcanic fluid input, crater topography, precipitation inflow, and seepage outflow on the lake system. We choose moderate atmospheric conditions, with an air temperature T_a = 10°C, relative humidity of 80%, air pressure $P_a = 8.8 \times 10^4$ Pa, and wind speed u = 2 m s^{-1}, all of which are constant in this analysis. It is noted that wind speed affects the magnitude of forced convection, especially in cases where the water temperature is much higher than the ambient air temperature (see Appendix). The moderate atmospheric conditions introduced here are a representative example of such a scenario.

Surface area is a key parameter in determining the total heat flux from the lake surface [*Pasternack and Varekamp*, 1997]. To demonstrate the relationship clearly, variations in the level and temperature of the crater lake can be analyzed in the following simple manner.

We assume that water volume V is proportional to lake level h; i.e.,

$$V = kSh, \tag{5}$$

where k is a constant.

Since lake size is a case-by-case parameter, we introduce dimensionless variables as follows. Let us consider a constant bottom input ($m = m_0$ and $H = H_0$). We then have

$$h = h_0\tilde{h}, \quad S = S_0\tilde{S}, \quad T = T_a\tilde{T}, \quad \varphi_e = \varphi_{e0}\tilde{\varphi}_e, \quad \Phi = \varphi_{e0}\tilde{\Phi}, \quad t = \frac{k\rho S_0 h_0}{m_0}\tilde{t}, \tag{6}$$

where h_0, S_0, and φ_{e0} correspond to the initial values of each parameter. Choosing $\tilde{t}$ as an independent variable, the following dimensionless equations are obtained:

$$\frac{d}{d\tilde{t}}\left(\tilde{S}\tilde{h}\right) = 1 - \frac{\tilde{\varphi}_e\tilde{S}}{\mu} - \frac{\tilde{S}\tilde{h}}{\lambda} + \frac{1}{\gamma}, \tag{7}$$

$$\frac{d}{d\tilde{t}}\left(\tilde{S}\tilde{h}\tilde{T}\right) = \varepsilon - \frac{L}{C_{pw}T_a\mu}\Phi\tilde{S} - \frac{\tilde{S}\tilde{h}\tilde{T}}{\lambda} + \frac{1}{\gamma}, \tag{8}$$

where μ is the ratio of bottom input mass to evaporative mass, ε is the ratio of bottom input enthalpy to lake water enthalpy, λ is the ratio of bottom input mass to seepage output mass, and γ is the ratio of bottom input mass to precipitation input mass:

$$\mu = \frac{m_0 L}{S_0 \varphi_{e0}}, \quad \varepsilon = \frac{H_0}{C_{pw} T_a}, \quad \lambda = \frac{m_0}{i\rho h_0 S_0}, \quad \gamma = \frac{m_0}{pfS_0}. \tag{9}$$

The dimensionless parameters μ, ε, λ, and γ represent factors that control the behaviors of water level and temperature of hot crater lakes. Based on equations (6)−(9), a timescale of a crater lake system is dominated by the ratio of lake water mass to the mass flux of fluid injected from the lake bottom, corresponding to the residence time [*Taran and Rouwet*, 2008], which is an important parameter in determining the rate of change in lake water chemical concentrations, water level, and temperature.

We calculate temporal variations in the dimensionless water level $\widetilde{h}$ and dimensionless temperature $\widetilde{T}$ using a fourth-order Runge-Kutta scheme. In the following sections, the behaviors of $\widetilde{T}$ and $\widetilde{h}$ are examined under given conditions of μ, ε, λ, and γ for a constant bottom input. The initial values of $\widetilde{h}$ and $\widetilde{T}$ are set to 1.

3. Numerical Analyses

3.1. Crater With a Cylindrical Topography

For a crater with a cylindrical topography, $k = 1$ and $\widetilde{S} = 1$. Therefore, equations (7) and (8) can be rewritten as follows:

$$\frac{d\widetilde{h}}{d\widetilde{t}} = 1 - \frac{\widetilde{\varphi}_e}{\mu} - \frac{\widetilde{h}}{\lambda} + \frac{1}{\gamma} \tag{10}$$

$$\frac{d}{d\widetilde{t}}\left(\widetilde{h}\widetilde{T}\right) = \varepsilon - \frac{L}{C_{pw} T_a \mu}\widetilde{\Phi} - \frac{\widetilde{h}\widetilde{T}}{\lambda} + \frac{1}{\gamma}. \tag{11}$$

Rigorous cylindrical topographies do not exist at real volcanoes; the cylindrical shape in the present model assumes a crater lake surrounded by a steep crater wall. Representative cases of this lake style include Yugama crater lake at Kusatsu-Shirane volcano, Japan [*Ohba et al*., 1994]; Laguna Caliente crater lake at Poás volcano, Costa Rica [*Tassi et al*., 2009]; and Yudamari crater lake at Aso volcano, Japan [*Terada et al*., 2008]; Rincon de la Vieja, Costa Rica [*Kempter and Rowe*, 2000; *Tassi et al*., 2005]; and Copahue on the Chile-Argentina border [*Tamburello et al*., 2015].

3.1.1. Responses of μ and ε to Lake Temperature and Level

In solving equations (10) and (11), Figure 2 shows temporal variations in the dimensionless temperature $\widetilde{T}$ and water level $\widetilde{h}$. We show five representative results, with ε = 30, 60, 77, 100, and 130; μ is set to 200 in all five simulations. Figure 2a assumes $\lambda = \infty$ and $\gamma = \infty$; i.e., seepage output and precipitation inflow are negligible relative to the bottom input mass m_0. An initial value of $\widetilde{T} = 1$ corresponds to an initial water temperature of T_a; i.e., water temperature = air temperature (Table 1).

$\widetilde{T}$ increases with increasing (dimensionless) time $\widetilde{t}$ because the enthalpies of the fluids injected from the lake bottom H_0 are higher than that of the lake water (equation (9)). $\widetilde{T}$ increases until the energy of the surface output is balanced by that of the bottom input. Finally, the water temperature becomes constant, indicating that energy equilibrium has been achieved. Hereafter, the constant temperature is referred to as $\widetilde{T}_c$.

Even in the case where a hot crater lake attains energy equilibrium, mass equilibrium is not always achieved. Figure 2 shows that the value of $\widetilde{h}$ changes over time (i.e., evaporative mass is not balanced by bottom input mass), even in the case that $\widetilde{T}_c$ is attained. The $\widetilde{h}$ increases with a small ε because the bottom input mass exceeds the evaporative mass. Conversely, evaporative mass exceeds bottom input mass under conditions where ε is large because a higher value of $\widetilde{T}_c$ is attained. Consequently, the parameter ε results in an increase in the temperature of the hot crater lake and limits any increase in lake level.

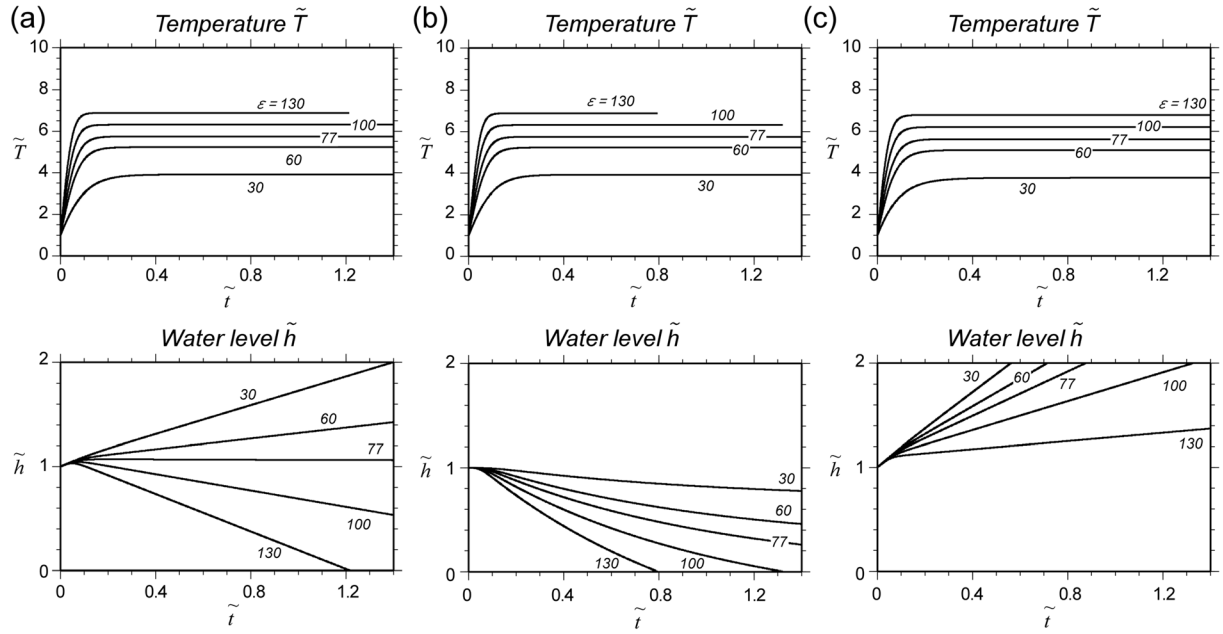

Figure 2. Computed dimensionless water temperature $\tilde{T}$ and level $\tilde{h}$ with a cylindrical topography (Figure 1a). We show five sets of results per pair of subfigures, corresponding to ε = 30, 60, 77, 100, and 130, with μ = 200 (see text for parameter descriptions). Atmospheric conditions are constant during calculations: air temperature T_a = 10°C, relative humidity is 80%, air pressure $P_a = 8.8 \times 10^4$ Pa, and wind speed u = 2 m s^{-1}. (a) $\lambda = \infty$ and $\gamma = \infty$; i.e., seeping output and precipitation input are negligible. (b) λ = 1 (seepage mass = bottom input mass) and $\gamma = \infty$. (c) $\lambda = \infty$ and γ = 1 (precipitation mass = bottom input mass).

Depending on ε, the dimensionless parameter μ affects the lake water level. Figure 3 shows the constant temperature $\tilde{T}_c$ (represented by the color scale) as a function of ε and μ, obtained numerically from equations (10) and (11). Here λ and γ are both set to ∞. Temperature $\tilde{T}_c$ increases with increasing ε and μ because the energy input increases with m_0 and H_0. Figure 3 also shows $d\tilde{h}/d\tilde{t}$ contours in the case where water temperature reaches $\tilde{T}_c$. If ε is large, evaporation is enhanced because of the high $\tilde{T}_c$; $\tilde{h}$ decreases with increasing μ (arrow A in Figure 3). In contrast, for a small value of ε, $\tilde{h}$ increases with increasing μ because smaller $\tilde{T}_c$ results in weak evaporation (Figure 3, arrow B).

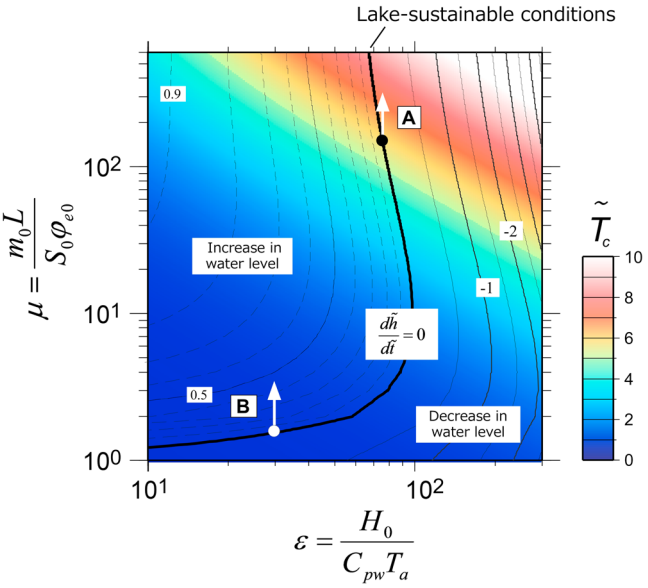

Figure 3. Constant temperature $\tilde{T}_c$ (color) and $d\tilde{h}/d\tilde{t}$ (contours) when water temperature reaches $\tilde{T}_c$. Crater topography is assumed to be a cylindrical shape. Seeping output and precipitation inflow are negligible relative to the bottom input mass m_0 (i.e., $\lambda = \infty$ and $\gamma = \infty$). Lake-sustainable conditions are represented by the line $d\tilde{h}/d\tilde{t}$ = 0, meaning mass and energy equilibria are simultaneously achieved. We discuss the behavior of the water level in section 3.1.1 using the examples denoted by arrows A and B.

The $d\tilde{h}/d\tilde{t}$ = 0 contour in Figure 3 represents the conditions necessary for mass and energy equilibria in the lake system, i.e., lake-sustainable conditions. In these cases, crater lakes can persist on long timescales.

3.1.2. Responses of λ and γ to Lake Temperature and Level

The dimensionless parameters λ and γ determine the impacts of seepage outflow and precipitation inflow on lake level, respectively (equation (9)). Figure 2b shows changes in lake level

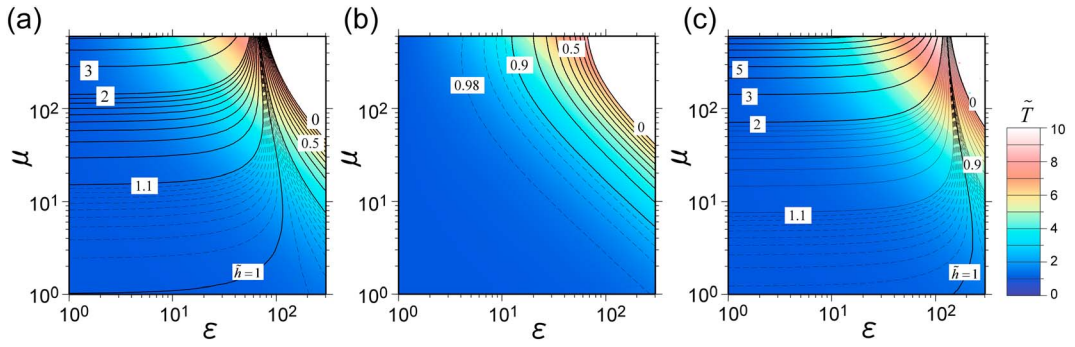

Figure 4. Model calculations showing dimensionless temperature $\tilde{T}$ (color shading) and dimensionless water level $\tilde{h}$ (contours) after 100 days. Crater topography is assumed to be cylindrical. The lake-sustainable conditions are largely consistent with the line $\tilde{h}=1$. (a) $\lambda=\infty$ and $\gamma=\infty$; i.e., seeping flux and precipitation inflow are negligible. (b) $\lambda=1$ and $\gamma=\infty$; i.e., the masses of seepage and bottom input are identical. (c) $\lambda=\infty$ and $\gamma=1$; i.e., the mass of precipitation is the same as that of the bottom input.

and temperature for $\lambda=1$ and $\gamma=\infty$, i.e., when the seepage output mass is equal to the bottom input mass. Figure 2c shows the changes for $\lambda=\infty$ and $\gamma=1$, i.e., when the bottom input mass is equal to the precipitation inflow mass.

Seepage outflow acts against increases in water level but has no effect on water temperature (Figure 2b). Precipitation inflow causes an increase in lake level, and inflow at air temperature T_a (equation (2)) causes a slight decrease in lake temperature relative to the case shown in Figure 2a.

When seepage outflow relative to bottom input mass is nonnegligible, $d\tilde{h}/d\tilde{t}$ varies, even though water temperature attains $\tilde{T}_c$ (Figure 2b). This occurs because seepage outflow is a function of water level (equation (3)). Therefore, instead of $\tilde{T}_c$ and $d\tilde{h}/d\tilde{t}$, we plot the dimensionless water temperature $\tilde{T}$ and level $\tilde{h}$ at a model time of 100 days ($t=8.64\times10^6$ s) under three sets of conditions: $\lambda=\infty$ and $\gamma=\infty$ (Figure 4a), $\lambda=1$ and $\gamma=\infty$ (Figure 4b), and $\lambda=\infty$ and $\gamma=1$ (Figure 4c). Results in Figure 4a, where seepage and precipitation flows are negligible, are essentially the same as in Figure 3a. Figure 4b shows that $\tilde{T}$ behaves similarly to that in Figure 4a, while $\tilde{h}$ shows no increase for the given values of μ and ε, due to seepage output. In the case that the mass of the seepage output is greater than or equal to the bottom input, the lake is unsustainable; hence, the lake-sustainable line does not exist (Figure 4b). A significant increase in $\tilde{h}$ (Figure 4c) occurs with a low ε value because of additional mass from precipitation inflow.

The lake-sustainable conditions are largely consistent with the line $\tilde{h}=1$. Precipitation inflow shifts the lake-sustainable line to a region of higher ε (Figure 4c). Conversely, seepage output acts to restrict the lake-sustainable line to lower ε. The effects of combined seepage and precipitation reduce or cancel one another.

3.2. Crater With a Conical Topography

Mass and heat are transferred from the lake surface; hence, crater geometry has an important effect on changes in water level and temperature [*Pasternack and Varekamp*, 1997]. In this section, we consider a conical crater for simplicity. In this case, $k=1/3$ in equation (5) and the surface area of the lake are proportional to the square of the water level:

$$S=h^2[\tan(90-\theta)]^2, \tag{12}$$

where θ is the slope angle measured from the horizontal (Figure 1b). The dimensionless lake surface area $\tilde{S}$ is defined by

$$\tilde{S}=\tilde{h}^2 \tag{13}$$

Using equation (13), equations (7) and (8) can be rewritten as

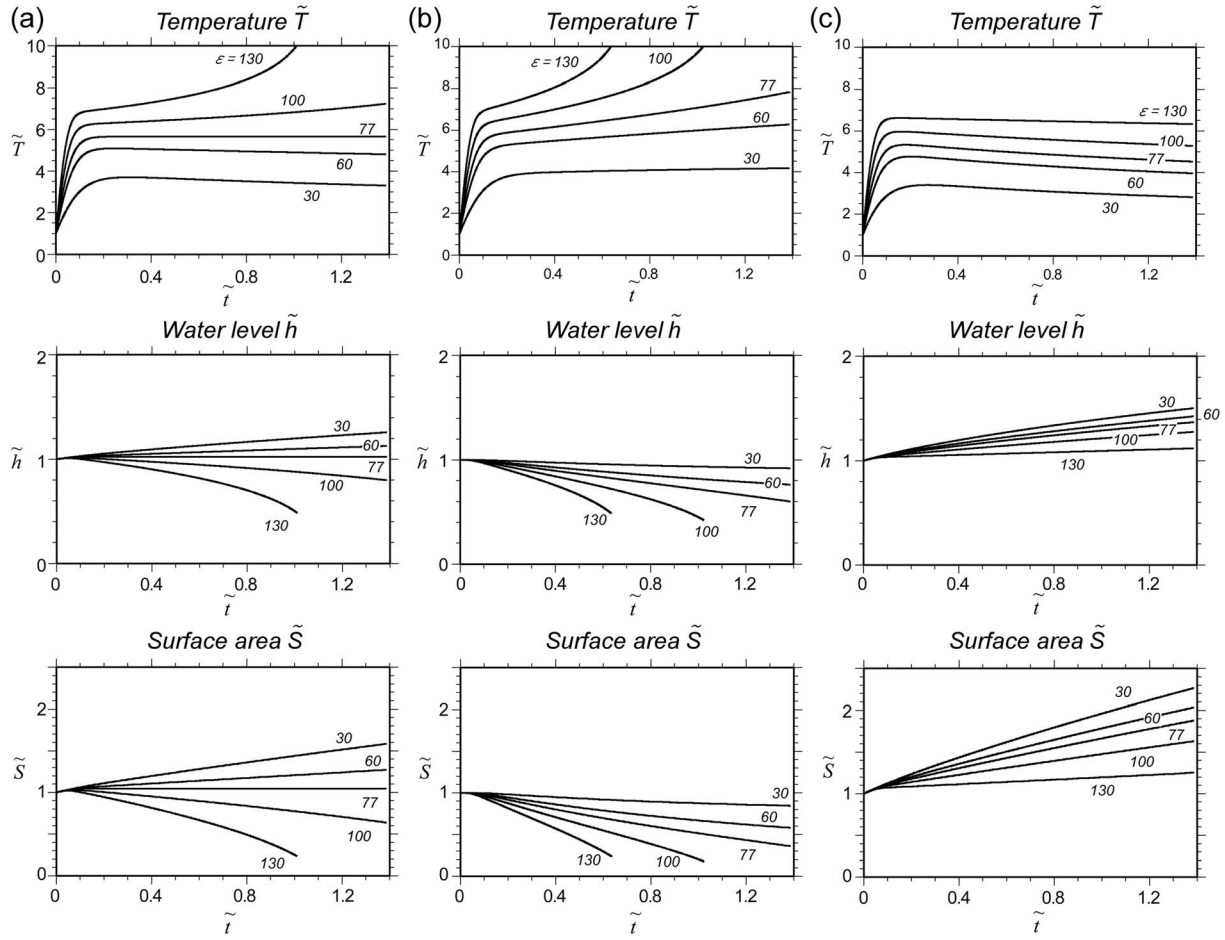

Figure 5. Computed dimensionless water temperature $\widetilde{T}$, level $\widetilde{h}$, and surface area $\widetilde{S}$ for crater lakes with conical topographies. The five sets of sample results shown correspond to ε = 30, 60, 77, 100, and 130, with the parameter μ = 200 (see text for definitions and explanations). Atmospheric conditions are constant during calculations. Computations are ended if the dimensionless water temperature $\widetilde{T}$ exceeds 10, corresponding to 100°C under conditions with T_a = 10°C. (a) $\lambda = \infty$ and $\gamma = \infty$; i.e., seeping output and precipitation input are negligible. (b) λ = 1 and $\gamma = \infty$; i.e., the seepage and bottom input masses are equal. (c) $\lambda = \infty$ and γ = 1; i.e., the precipitation mass is the same as the bottom input mass.

$$\frac{d\widetilde{h}^3}{d\widetilde{t}} = 1 - \frac{\widetilde{\varphi}_e\widetilde{h}^2}{\mu} - \frac{\widetilde{h}^3}{\lambda} + \frac{1}{\gamma}, \tag{14}$$

$$\frac{d}{d\widetilde{t}}\left(\widetilde{h}^3\widetilde{T}\right) = \varepsilon - \frac{L}{C_{pw}T_a\mu}\widetilde{\Phi}\widetilde{h}^2 - \frac{\widetilde{h}^3\widetilde{T}}{\lambda} + \frac{1}{\gamma}. \tag{15}$$

Representative examples of crater lakes with conical topographies include Kawah Ijen, Indonesia [*Takano et al.*, 2004], Ruapehu, New Zealand [*Christenson*, 1994], and El Chichón, Mexico [*Rouwet*, 2011].

3.2.1. Response of μ and ε to Lake Temperature and Level

Figure 5 shows temporal variations in dimensionless water temperature $\widetilde{T}$, lake level $\widetilde{h}$, and surface area $\widetilde{S}$. As in Figure 2, we show five sets of results, using ε = 30, 60, 77, 100, and 130; μ is set to 200.

Figure 5a assumes $\lambda = \infty$ and $\gamma = \infty$; i.e., seepage output and precipitation inflow are negligible relative to bottom input mass m_0. Although the enthalpy H_0 and mass m_0 of the fluids injected from the lake bottom are invariant, the water temperature $\widetilde{T}$ in Figure 5a continues to change over time because the surface area $\widetilde{S}$ changes with $\widetilde{h}$, which is in contrast to the result for a cylindrical crater (Figure 2a). A decrease in water level $\widetilde{h}$ results in an increase in water temperature $\widetilde{T}$ due to reduced energy output, leading to a further decrease in $\widetilde{h}$ and increase in temperature $\widetilde{T}$. In contrast, an increase in water level $\widetilde{h}$ leads to a decrease in temperature and a slight additional increase in $\widetilde{h}$.

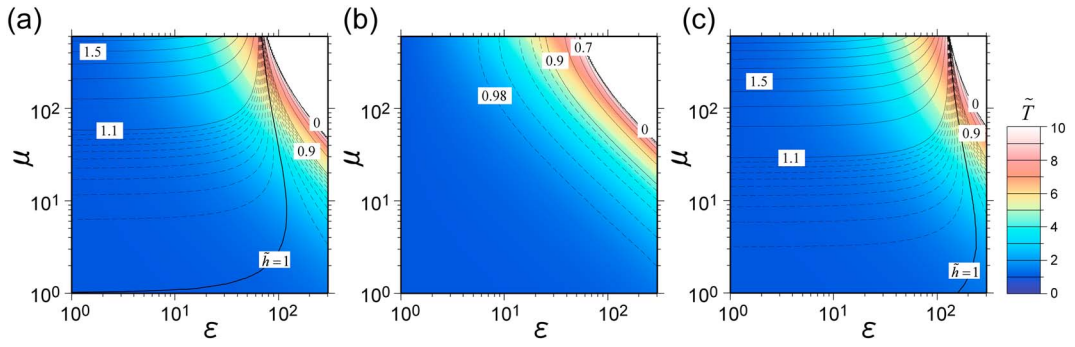

Figure 6. Model calculations showing dimensionless temperature $\tilde{T}$ (color shading) and water level $\tilde{h}$ (contours) at a model time of 100 days. Crater topography is assumed to be a circular-conical shape. The lake-sustainable conditions are largely consistent with the line $\tilde{h}=1$. (a) $\lambda=\infty$ and $\gamma=\infty$; i.e., seeping flux and precipitation inflow are negligible. (b) $\lambda=1$ and $\gamma=\infty$; i.e., the masses of the seepage and bottom input are equal. (c) $\lambda=\infty$ and $\gamma=1$; i.e., the mass of precipitation is the same as that of the bottom input.

Figure 6a shows dimensionless temperature $\tilde{T}$ and water level $\tilde{h}$ at a model time of 100 days ($t = 8.64 \times 10^6$ s) under $\lambda=\infty$ and $\gamma=\infty$. As with the cylindrical crater (Figure 4), $\tilde{T}$ increases with increasing ε and μ due to an increase in energy input. The $\tilde{h}$ increases with μ at small values of ε, while $\tilde{h}$ decreases with μ at large ε.

Compared with the case of a cylindrical crater (Figure 4), a conical crater results in less severe increases in $\tilde{h}$ at lower ε and a greater decrease in $\tilde{h}$ at higher ε, because the lake surface area $\tilde{S}$ changes with $\tilde{h}$. The $\tilde{h}=1$ contour in Figure 6 largely agrees with the conditions of mass and energy equilibria in the lake system; i.e., lake-sustainable conditions are achieved.

3.2.2. Response of λ and γ to Lake Temperature and Level

In the case of conical topography, increased seepage output can raise the water temperature and increased precipitation can decrease it. Figure 6b shows temporal variations in $\tilde{h}$ and $\tilde{T}$ for $\lambda=1$ and $\gamma=\infty$, i.e., when seepage outflow is equal to bottom input mass m_0 and while precipitation inflow is negligible relative to m_0. Figure 6c shows the case for $\lambda=\infty$ and $\gamma=1$, i.e., when precipitation inflow is equal to m_0 and while seepage outflow is negligible relative to m_0. An increase in the dimensionless parameter λ leads to a rise in temperature (Figures 5b and 6b) because seepage decreases the water level and hence the lake's surface area. Finally, evaporative energy decreases, resulting in a further increase in temperature, even though the mass and enthalpy of the fluid injected from the lake bottom are invariant. Conversely, an increase in γ leads to a decrease in temperature, because precipitation influx increases the water level and surface area of the lake (Figures 5c and 6c).

In Figure 6c, increased precipitation inflow results in a shift in the lake-sustainable condition to a region with larger ε (Figure 6a). Seepage output acts to restrict the lake-sustainable conditions to smaller ε values (Figure 6b) than without seepage. When the mass of the seepage output is greater than or equal to that of bottom input, the lake cannot be sustained; hence, the lake-sustainable condition does not exist (Figure 6b).

Table 2. Summary of the Factors That Control Water Level and Temperature, as Suggested by the Numerical Investigations of Section 3

Factor	Topography	Water Temperature	Water Level
ε (bottom input enthalpy/lake water enthalpy)	Cylindrical	↑	↓
	Conical		
μ (bottom input mass/evaporative mass)	Cylindrical	↑	Depends on other parameters
	Conical		
λ (bottom input mass/seepage output mass)	Cylindrical	No effect	↑
	Conical	↓	
γ (bottom input mass/precipitation input mass)	Cylindrical	Minor effect	↓
	Conical	↑	

3.3. Summary of Influences of ε, μ, λ, and γ on Lake Level and Temperature

The factors that control water level and temperature are summarized in Table 2. An increase in the dimensionless parameter ε, which is proportional to the bottom input enthalpy H_0 (equation (9)), increases water temperature, which leads to a decrease in water level due to enhanced evaporation.

An increase in the dimensionless parameter μ (equation (9)) causes an increase in water temperature; however, the behavior of the water level is controlled by ε (Figures 3, 4, and 6). When ε is small, resulting in minor evaporation at low water temperature, the water level $\widetilde{h}$ increases with increasing μ (m_0/S_0) (arrow B in Figure 2). In contrast, when ε is large, $\widetilde{h}$ decreases with μ at higher water temperatures (arrow A in Figure 2).

A decrease in the dimensionless parameter λ, corresponding to an increase in seepage output (equation (9)), decreases the water level (Figure 2b). In the case of a conical crater (Figure 5b), where the lake surface area changes with a change in water level, a decrease in λ can cause a rise in water temperature due to the decreased surface area. Thus, an increase in seepage rate leads to further decreases in water level, even though the fluid injected from the lake bottom rate is unchanged.

A decrease in the dimensionless parameter γ, corresponding to an increase in precipitation input (equation (9)), causes an increase in the water level (Figure 2c). In the case of a conical crater (Figure 5c), a decrease in γ decreases water temperature, due to the increased lake surface area. Hence, increasing the precipitation rate decreases the water temperature and increases the water level.

The specific range of H_0 in which hot crater lakes can be maintained depends on the seepage output parameter λ and the precipitation input parameter γ: a decrease in λ restricts the lake-sustainable line to a smaller value of ε (H_0) (Figures 4b and 6b), whereas a decrease in γ shifts the lake-sustainable line to a larger value of ε (H_0) (Figures 4c and 6c). Both λ and γ are nonnegligible for most real crater lakes; however, the effects of λ and γ reduce or cancel one another.

4. Stability of Lake-Sustainable Conditions

Perturbations in water level and temperature can be caused by temporary increases/decreases in subaqueous thermal activity. In addition, nonthermal activity (e.g., heavy rain and anomalously low precipitation during the rainy season) can cause short-term perturbations in the water level and temperature.

Here we assess the stability of crater lake water levels and temperatures under sustainable conditions with respect to perturbations in water level and temperature. For these analyses, we select three pairs of ε and μ that generate lake-sustainable conditions. The moderate atmospheric conditions described in section 2.4 remain constant throughout these analyses. Seepage output and precipitation input are negligible relative to bottom input mass here ($\lambda = \infty$ and $\gamma = \infty$), because these parameters are not essential problems in these cases.

To assess the stability of the water level, we show $d\widetilde{h}/d\widetilde{t}$ and $d\widetilde{T}/d\widetilde{t}$ as a function of $\widetilde{h}$ and $\widetilde{T}/\widetilde{T}_c$, whereas other parameters remain constant; $\widetilde{T}_c$ is a constant temperature when energy equilibrium is achieved, as defined in section 3.1. $\widetilde{T}$ is normalized by $\widetilde{T}_c$ because the constant temperature $\widetilde{T}_c$ also varies with ε and μ.

4.1. Cylindrical Topography

A system in mass and energy equilibrium is stable with respect to perturbations in water level and temperature for a cylindrical topography; the lake surface area does not change with water level.

Figures 7a and 7b show $d\widetilde{h}/d\widetilde{t}$ and $d\widetilde{T}/d\widetilde{t}$ as functions of $\widetilde{h}$, respectively. Temporal variations in $d\widetilde{h}/d\widetilde{t}$ and $d\widetilde{T}/d\widetilde{t}$ remain constant as $\widetilde{h}$ changes, showing that mass and energy equilibria are unaffected by perturbations in the water level. Figures 7c and 7d show $d\widetilde{h}/d\widetilde{t}$ and $d\widetilde{T}/d\widetilde{t}$ as functions of $\widetilde{T}/\widetilde{T}_c$, respectively. An increase (decrease) in water temperature results in a decrease (increase) in water level (Figure 7c) due to an increase (decrease) in evaporative mass.

Figure 7d implies that the water temperature is stable with respect to temperature perturbations due to negative feedback effects: a rise (fall) in water temperature causes an increase (decrease) in evaporative energy, and thereby decreases (increases) temperature. In fact, evaporation is an efficient cooling mechanism

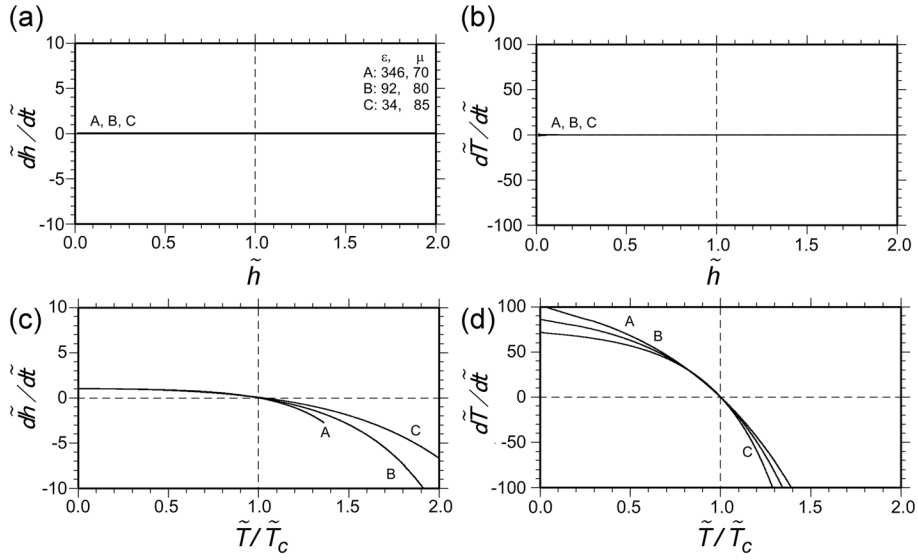

Figure 7. Stability tests of a crater lake with a cylindrical topography, showing (a) $d\tilde{T}/d\tilde{t}$ and (b) $d\tilde{h}/d\tilde{t}$ as functions of $\tilde{T}/\tilde{T}_c$, and (c) $d\tilde{T}/d$ and (d) $d\tilde{h}//d\tilde{t}$ as functions of $\tilde{h}$. Three pairs of ε and μ (represented by A−C) are shown, in which lake sustainable conditions are achieved. Seepage and precipitation mass are negligible relative to bottom input mass (i.e., $\lambda = \infty$ and $\gamma = \infty$).

for heated water bodies. As a result, the water temperature $\tilde{T}$ returns to $\tilde{T}_c$ under each of the given values of ε and μ, resulting in a stable water level.

4.2. Conical Topography

We note that the surface area of a crater lake changes with water level, in the case of a conical crater. This implies that the conditions required for mass and energy equilibria also change with changes in water level, leading to shrinkage of hot crater lakes without any change in subaqueous fumarolic activity.

Figures 8a and 8b show $d\tilde{h}/d\tilde{t}$ and $d\tilde{T}/d\tilde{t}$ as functions of $\tilde{h}$. The water level is stable with respect to perturbations in lake level (Figure 8a), while an increase (decrease) in temperature is caused by a decrease (increase) in water level (Figure 8b) due to a decrease (increase) in surface area, leading to a decrease (increase) in evaporation energy loss rate.

Figures 8c and 8d show $d\tilde{h}/d\tilde{t}$ and $d\tilde{T}/d\tilde{t}$ as functions of $\tilde{T}/\tilde{T}_c$. An increase (decrease) in temperature causes a decrease (increase) in lake level and a corresponding decrease (increase) in temperature, as in the case of a cylindrical crater (Figures 7c and 7d).

Of note, a decrease in water level results in increasing temperature (Figure 8b), in contrast to crater lakes with cylindrical topographies (Figure 7b). In such a situation, a decrease in water level leads to a further decrease in water level (Figure 8c). This positive feedback effect causes shrinkage of the crater lake even though the fluid injected from the lake bottom does not change. Conversely, an increase in water level leads to a decrease in temperature and a further, albeit minor, increase in water level.

Consequently, when the surface area of the crater lake changes with water level, a hot crater lake is unstable with respect to perturbations in water level and water temperature. In contrast, when the lake surface area is near-constant with respect to changes in lake level, a hot crater lake under sustainable conditions is stable with respect to perturbations in water level and/or temperature (Figure 7).

5. Discussion

Given appropriate parameters (represented here by m_0/S_0 and H_0) along the lake-sustainable line, under conditions that include seepage output and precipitation input, mass and energy equilibria in the lake system are simultaneously achieved. In such cases, crater lakes can persist on relatively long timescales. This result suggests that neither a high precipitation rate nor an impermeable layer beneath a lake bottom is always necessary for the long-term persistence of hot crater lakes, as long as the values of m_0 and H_0 are

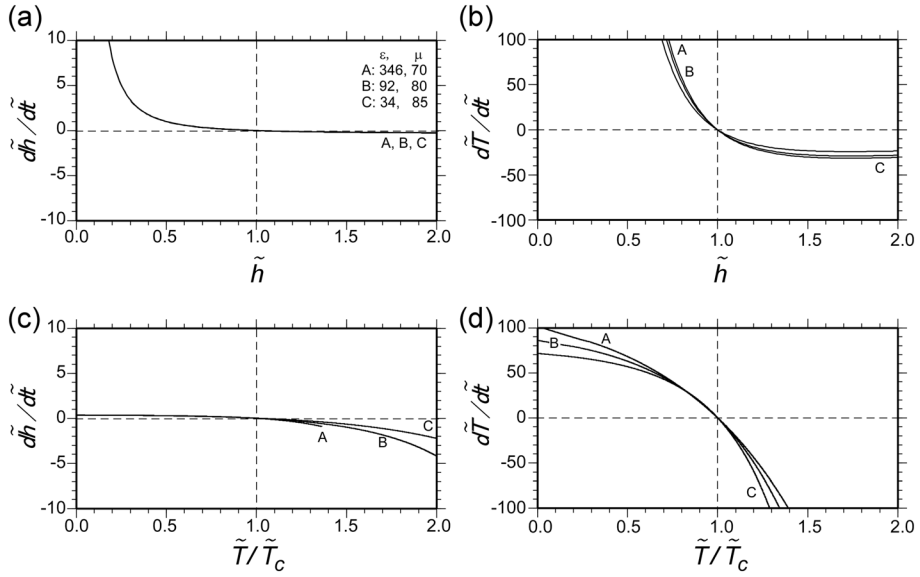

Figure 8. Stability tests of a crater lake with a conical topography, showing (a) $d\tilde{T}/d\tilde{t}$ and (b) $d\tilde{h}/d\tilde{t}$ as functions of $\tilde{T}/\tilde{T}_c$, and (c) $d\tilde{T}/d\tilde{t}$ and (d) $d\tilde{h}/d\tilde{t}$ as functions of $\tilde{h}$. Three pairs of ε and μ (labeled A−C in the subfigures) are shown, each of which maintains lake-sustainable conditions. Seepage and precipitation mass are negligible relative to bottom input mass (i.e., $\lambda = \infty$ and $\gamma = \infty$).

appropriate for the crater topography. Impermeable layers of altered material are commonly seen at geothermal systems, but this does not appear to be a requirement to form persistent hot crater lakes.

The lake-sustainable line is roughly an inverted L shape in all of our simulations (Figures 3, 4, 6, and 9). Therefore, high-temperature crater lakes can be maintained under conditions that include seepage and precipitation if the bottom input enthalpy H_0 falls within a specific range. In the case of high-temperature crater lakes, a temporary shift from the lake-sustainable line can cause nonnegligible changes in lake level because the timescales (residence times) are relatively small for larger values of m_0/S_0 (see equation (6)). They explain why high-temperature crater lakes are rare compared with other-crater lake types.

Assuming a bottom input enthalpy of ~4200 kJ/kg, *Pasternack and Varekamp* [1997] reported that a hot crater lake with a high temperature (>40−50°C) requires an average rainfall of over 5 m/year. Our results suggest that neither a high precipitation inflow nor an impermeable zone at the lake bottom is always necessary to maintain a hot crater lake in the long term. Indeed, Yudamari crater lake, at Aso volcano, Japan, maintains lake water temperatures of over 60–70°C during noneruptive periods in an area with annual rainfall always less than 5 m, with nonnegligible seepage outflow [*Terada et al*., 2012].

In the remainder of this section, we discuss the conditions that support the existence of hot crater lakes, a classification system for crater lakes based on numerical considerations, precursory signals of eruptions at crater lakes, and applications to actual hot crater lakes.

5.1. Varieties of Volcanic Lakes

Crater lakes show considerable variety in water temperature, lake size, pH, TDS (g/L), and chemical composition. Our model suggests that variety can be explained by differences in m_0/S_0 and H_0, based on the present numerical investigation.

5.1.1. Classification of Crater Lakes Based on Numerical Results

A classification scheme for crater lakes was proposed by *Pasternack and Varekamp* [1997] and *Rouwet et al*. [2014], on the basis of physical-chemical characteristics: the possible categories include low activity, medium activity, high activity, peak activity, and variable mass (erupting).

Low-activity lakes have low TDS (g/L) and low-temperature water; a representative case in this class is Okama crater lake at Zao volcano, Japan. *Medium-activity lakes* are underlain by an active hydrothermal system; as a result, water temperature is generally higher than ambient air temperature. The pH is low due to the

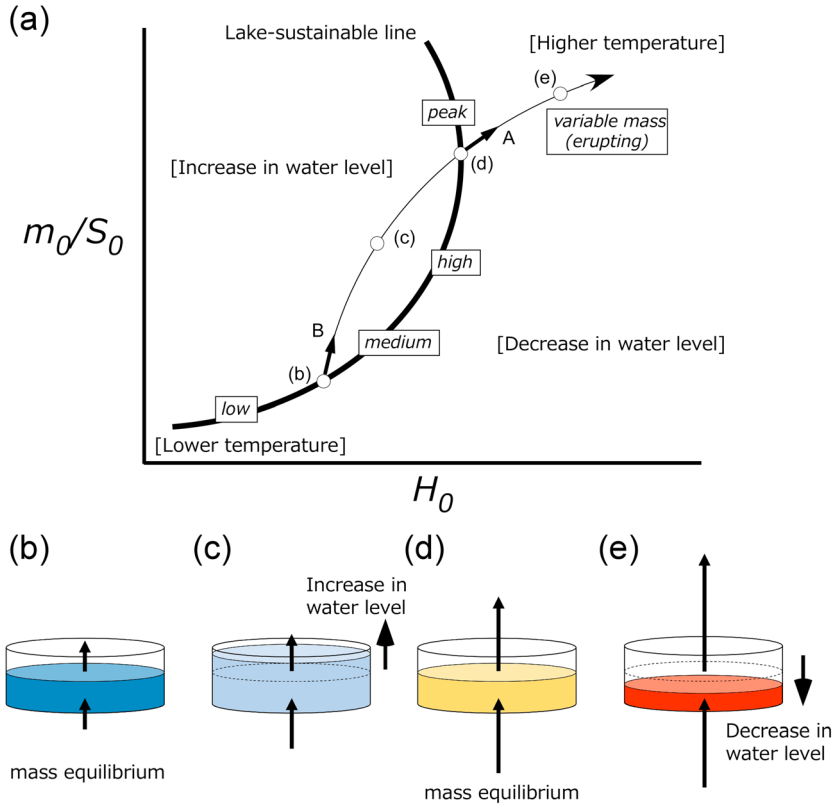

Figure 9. Summary of a variety of volcanic lakes. (a) Diagram of lake-sustainable conditions and patterns of change in water temperature and level. We discuss the behavior of water level in section 5.2 using the examples denoted by arrows A and B. (b–e) Illustrations of mass equilibria of volcanic lakes. Each set of volcanic lake conditions is denoted by letters b−e in Figure 9a. Arrows from lake bottoms and from lake surfaces represent fluid injection and evaporation mass, respectively.

oxidation of H_2S to SO_4 ions, while TDS (g/L) is not significantly high. The crater lakes of El Chichón, Mexico [*Rouwet et al.*, 2004], and Mount Pinatubo, Philippines, belong to this class. *High-activity lakes*, including the crater lakes of Kawah Ijen, Keli Mutu TiN, Indonesia, and the Yugama crater lake of Kusatsu-Shirane volcano, Japan, are characterized by powerful subaqueous fumarolic activity. High TDS (g/L) and low pH values are commonly observed, indicating the influence of acidic volatiles such as SO_2, HCl, and HF. Water temperatures are ~30°C. *Peak-activity lakes* have hyperacidic, highly saline water with a temperature of >45°C. Yudamari crater lakes at Aso volcano, Japan, and Laguna Calientes at Poás Volcano, Costa Rica, are two examples of *peak-activity lakes* [*Rouwet et al.*, 2014].

Crater lakes classed as *low-*, *medium-*, *high-*, and *peak-activity lakes* exist in a steady state, meaning that mass equilibrium is attained in these systems. We consider that the lake system of each crater lake lies roughly along the lake-sustainable line introduced in the present study (Figure 9a). The bottom input enthalpy H_0 and the ratio of bottom input mass to lake surface area, m_0/S_0, increase from *low-activity lakes* to *high-activity lakes*. An increase in H_0 corresponds to a rise in temperature or an increase in the average gas/liquid ratio among the fluids injected from the lake bottom, implying an increase in high-temperature fluids, such as magmatic acidic volatiles. Thus, the TDS (g/L) and water temperature of *medium-activity lakes* are both high compared with *low-activity lakes*.

Differences between *high-activity lakes* and *peak-activity lakes* can be explained by variations in m_0/S_0 as well as H_0. An increase in m_0/S_0 causes an increase in temperature that leads to the condensation of lake water, due to enhanced evaporation loss from the lake surface. Consequently, TDS (g/L) increases and pH decreases. Even if a small amount of m_0 is input, *peak-activity lakes* can exist with a small S_0.

Variable mass (erupting) lakes cannot be sustained in the long term without sufficient meteoric water recharge [*Pasternack and Varekamp*, 1997; *Rouwet et al.*, 2014], because evaporation loss exceeds mass

input from subaqueous fumaroles. With respect to the present work, we consider *variable mass (erupting) lakes* to exist above and to the right of the lake-sustainable line in Figure 9a. Under such conditions, crater lakes shrink, whereas temporary increases in water level can occur due to precipitation inflow. Consequently, variable mass changes in lake water are observed in this class. High-temperature fumaroles often occur adjacent to *variable mass (erupting) lakes* [*Rouwet et al*., 2014], consistent with the high enthalpy of the fluid injected from the lake bottom.

5.1.2. Two States of Mass Balance of Hot Crater Lakes

From the perspective of mass balance conditions, our model suggests two types of hot crater lakes. Figures 9b–9e illustrate the mass balance of lake water for various dimensionless parameters along the thin line shown in Figure 9a. A small mass flux of fluid injection is balanced by an evaporation mass at a low water temperature (Figure 9b). The water level increases because increased evaporation mass is insufficient to overcome the additional mass from subaqueous fumaroles (Figure 9c).

If larger m_0/S_0 and H_0 are given, mass equilibrium can be reattained. Under these conditions, a high mass flux of fluid injected from the lake bottom is balanced by enhanced evaporation loss due to the high water temperature (Figure 9d). As m_0/S_0 and H_0 continue to increase, mass equilibrium becomes impossible (Figure 9e).

5.2. Precursory Signals of Eruptions at Crater Lakes

Figure 9 is provided to interpret changes in volcanic activity based on the monitoring of crater lakes. Our numerical investigations indicate that a system's response to changes in subaqueous fumarolic activity depends on the class of its crater lake (section 5.1). Increases in m_0 and H_0 in a high-temperature crater lake, such as a *peak-activity lake* (e.g., arrow A in Figure 9a), clearly cause a decrease in water level, accompanied by a rise in temperature, meaning that the state of the lake shifts to a *variable mass (erupting) lake* (Figure 9e).

In contrast to the case of high-temperature crater lakes (e.g., *peak-activity lakes*), for low-temperature crater lakes (including *low-*, *medium-*, and some *high-activity lakes*) the water level can increase with an increase in bottom input mass m_0 and enthalpy H_0, as described in sections 3.1.1 and 5.1.2. (e.g., arrow B in Figures 9a and 9c). It is notable that the timescale (residence time) of *low-activity lakes* is large relative to that of other lakes. Changes in water level and temperature may be too slow to detect, so these crater lakes might show ambiguous precursory signals of eruptions.

Barberi et al. [1992] reported that increases in water temperature and lake level preceded phreatic eruptions at 17 of 19 crater lake case studies, whereas a rise in water temperature was accompanied by a decrease in water level in the remaining two cases. Our present model suggests that these differences in lake level behavior are caused by variety among crater lake systems in terms of mass and energy equilibria (see section 5.1.2).

Simultaneous increases in m_0 and H_0 are likely caused by pressurization and heating of the hydrothermal system beneath the crater lake, likely due to enhanced degassing of magma at depth. Such an increase in the degassing rate was detected by audiometric noise monitoring at Kelut crater lake, Indonesia [*Vandemeulebrouck et al*., 2000]. Analogue models suggest that increases in m_0 and H_0 may result from an expansion of the two-phase zone in the porous media beneath a crater lake [e.g., *Vandemeulebrouck et al*., 2005].

5.2.1. Decreases in Water Level Before Eruptions

We have observed decreases in crater lake water levels preceding eruptions at Yudamari crater lake that we interpret as *peak activity* (Figure 9). Figure 10 shows SO_2 flux emitted from the lake surface and nearby fumaroles, the monthly number of earthquakes, temporal changes in water level and temperature, and annual precipitation. Prior to a series of phreatomagmatic eruptions in 2014−2016, a significant decrease in water level and a rise in temperature occurred simultaneously in 2013 (red shading in Figure 10). Such dramatic changes in the Yudamari crater lake were accompanied by intense SO_2 emissions and microearthquake swarms, indicating increases in mass flux and enthalpy of subaqueous fumaroles due to enhanced degassing at depth. Further increases in m_0 and H_0 can cause a lake system to transition from a *peak-activity lake* to *variable mass (erupting) activity*, leading to the disappearance of the crater lake. Indeed, Yudamari crater lake was almost boiling dry between July 2014 and July 2016, although lake water was temporarily observed after heavy rains. The disappearance of Yudamari crater lake is a known precursor of eruptions at Aso volcano [*Terada et al*., 2012]. A similar pattern of lake behavior has been reported at Poás, Costa Rica [*Brown et al*., 1989; *Rowe et al*., 1992; *Rouwet et al*., 2016].

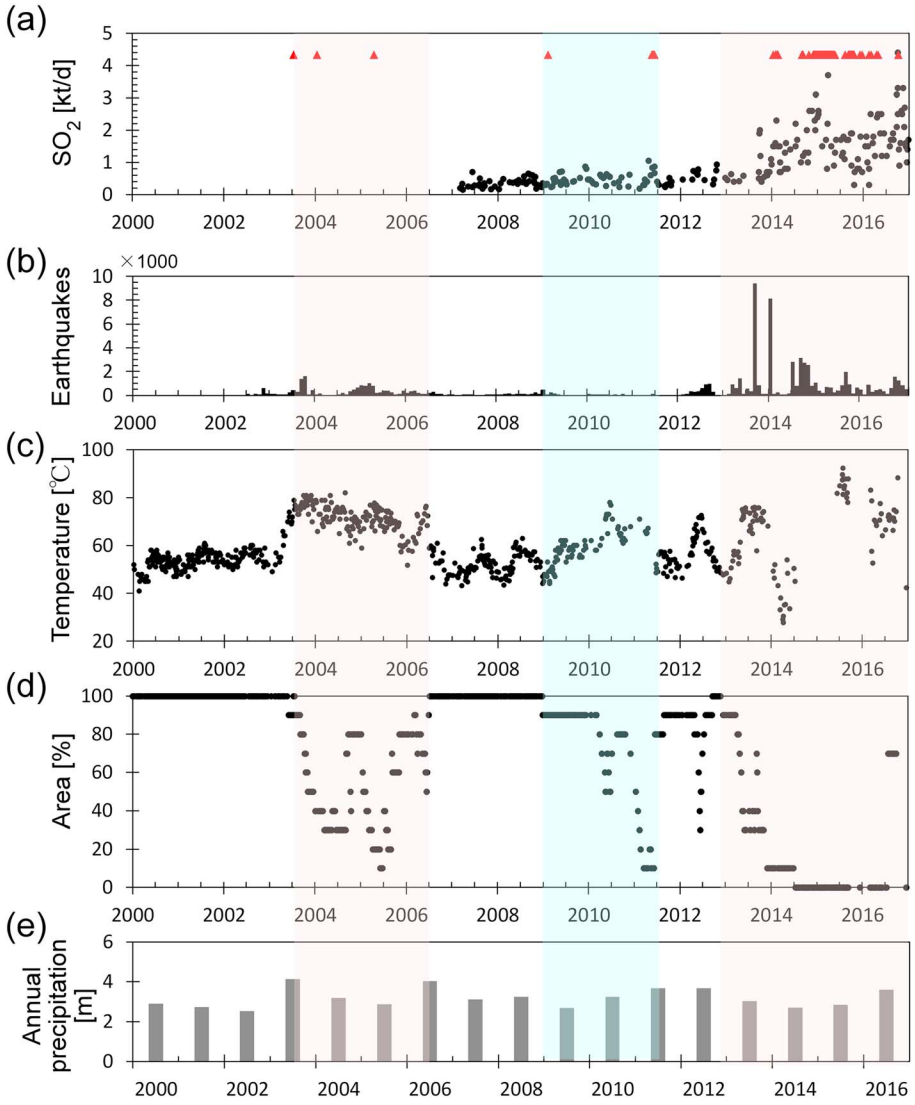

Figure 10. Japan Meteorological Agency (JMA) observation records for Aso volcano. (a) Temporal changes in SO_2 flux. The triangles represent dates of eruptions. (b) Monthly numbers of microearthquakes with maximum amplitudes on the UD component of the station "Nakadake Nishi Sanpuku," on the western slope of Nakadake (800 m west of Yudamari), of >3 μm. S-P times of events represented here were <3.0 s at this station. (c) Temporal changes in apparent lake surface temperature measured by IR thermometry. (d) Area of Yudamari crater lake as a percentage of the maximum area. (e) Annual precipitation measured at Aso Weather Station, located 1.2 km west of Yudamari crater lake. Areas in red and blue shading denote periods of shrinkage of the Yudamari crater lake (see sections 5.2.1 and 5.3.2 for details).

In a similar case to the behavior of Aso in 2013, a significant decrease in water level accompanied by a rise in lake temperature was observed between 2003 and 2006. During this period, *Fukuoka Regional Headquarters, Japan Meteorological Agency* [2016] reported SO_2 fluxes of 500–3000 t/d, which is several times higher than values reported during quiescent periods [*Miyabuchi and Terada*, 2009]. In addition, three eruption events [*Miyabuchi et al*., 2008] were accompanied by microearthquake swarms (Figure 10). Although the mass estimates of ejecta erupted during each event were small (1.2–4.2 t), we believe that lake shrinkage in 2002 was caused by an increase in mass flux and enthalpy of subaqueous fumaroles. The reason for the re-formation of Yudamari lake in July 2006 seems to be intense precipitation: the 2.1 m recorded in the rainy season of that year (June and July) was 1.6 times higher than in an average year (Figure 10). Subaqueous fumarolic activity returned to quiescent levels by the rainy season of 2006.

The shrinkage of Yudamari crater lake observed in 2010 was not accompanied by an increase in SO_2 flux or seismicity; this appears to have been only "apparent unrest" and will be discussed at section 5.3.

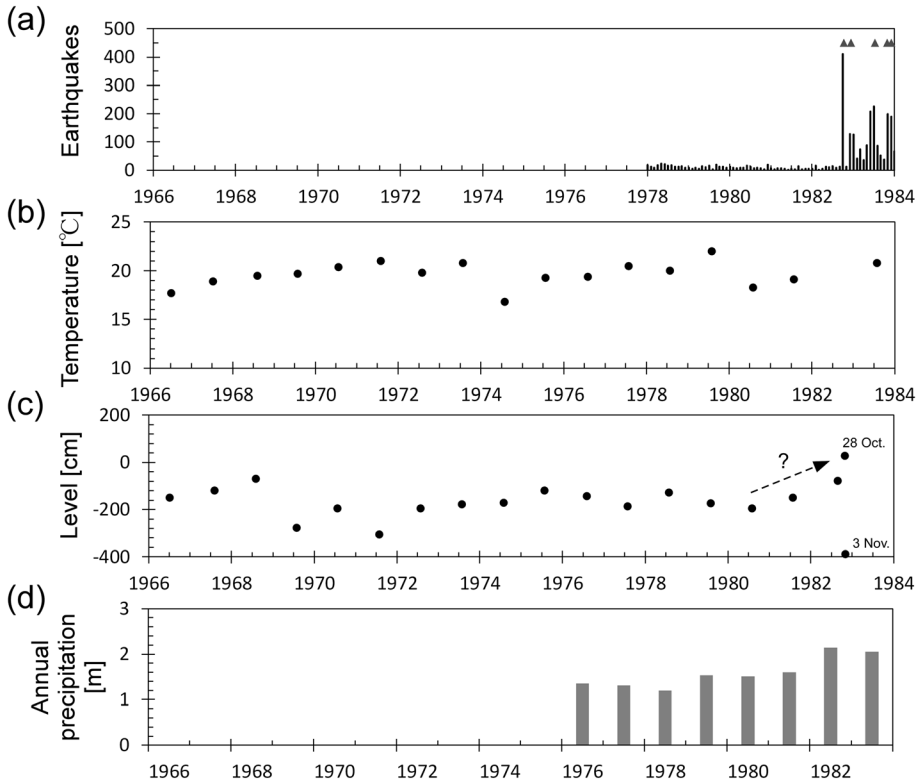

Figure 11. Observation records at Kusatsu-Shirane volcano. (a) Monthly numbers of microearthquakes with maximum amplitudes of >0.05 μm, S-P times of <2 s, and the UD component of seismic station "Mizugama Hokuto," 1 km northeast of Mizugama crater. Data were provided by the Japan Meteorological Agency (JMA). (b) Water temperature measured at the southern shore of Yugama crater lake in June or July of each year [after *Ohba et al*., 2008]. (c) Relative changes in the water level of Yugama crater lake, measured at almost the same time as water temperature [after *Tokyo Institute of Technology and Sophia University*, 1984]. The increase in water level on 28 October 1982 was followed by a rapid decrease in water level. A water level of −859 cm was measured on 28 January 1983 because the lake water drained to the new vent that formed on the northern shore of Yugama [*Tokyo Institute of Technology and Sophia University*, 1984]. (d) Annual precipitation at Kusatsu town, 6 km east of Yugama crater lake, as measured by JMA.

5.2.2. Increases in Water Level Before Eruptions

Increases in crater lake levels prior to eruptions were observed at Green lake, Raoul volcano, New Zealand in 1964 [*Healy et al*., 1965; *Christenson et al*., 2007]. Figure 11 shows water level, temperature, and seismicity data of Kusatsu-Shirane volcano (*high activity*; Figure 9) in Japan. Water level and temperature show seasonal changes, so the data in Figure 11 were measured during the summer season (July and August).

During the quiescent period at Yugama crater, from 1966 to 1980, water temperature and level were roughly constant. Preceding the 1982 eruption, a gradual increase in water level (60 cm/yr) was observed, whereas water temperature remained almost constant. After the first eruption of 26 October 1982, an increase in water level of 50 cm was measured on 28 October. Furthermore, 2 months before the eruption, concentrations of polythionates showed a marked decrease, which implies an increase in the SO_2/H_2S ratio of the subaqueous fumaroles [*Takano and Watanuki*, 1990]. These observations indicate that subaqueous fumarolic activity was enhanced. Consequently, we suspect that the status of the Yugama crater lake shifted to reflect an increase in water level (top left region of Figure 9a) preceding the onset of the 1982−1983 eruption sequence.

Variations in water levels are sensitive to fluctuations in annual precipitation; however, no precipitation data are available from the area around Yugama crater lake during this period (data presented in Figure 11d were recorded at Kusatsu town, 6 km east of Yugama crater lake). Seismic data are from 1978; we do not discuss reasons of fluctuations in water level around 1970 showing in Figure 11c.

5.3. Apparent Volcanic Unrest Due to Topographic Effects

The dimensionless parameter μ takes into account the lake surface area S_0 in the denominator and the bottom input mass m_0 in the numerator. It means that a reduction in lake size S_0 has the same effect as an increase in bottom input mass m_0. In such a situation, chemical concentrations and water temperature would increase, even if subaqueous fumarolic activity did not change. Such variations in crater lake properties are referred to here as "apparent volcanic unrest," which indicates only superficial (or benign) changes in volcanic activity.

5.3.1. Cylindrical Topography

Even if a crater has a cylindrical topography, a modification in lake size can occur due to landslide or erosion of the crater wall. In this section, we discuss the effects of changes in topography on the lake system.

If a *peak-activity lake* with a cylindrical topography maintains lake-sustainable conditions as in Figure 9a, then a decrease in S_0 (i.e., shrinkage of a crater lake) increases the water temperature and decreases the water level. Consequently, the hot crater lake is no longer maintained, and it transitions to the state of *variable mass (erupting) activity*. In such a situation, chemical concentrations and water temperature increase, and water level decreases until the lake disappears. One possible reason for a reduction in lake size without an accompanying change in the supply of the fluid injection is a landslide into the crater lake from the surrounding crater wall.

Conversely, an increase in S_0 (i.e., expansion) of a *peak-activity lake*, corresponding to a decrease in μ, reduces water temperature. In this situation, an increase in lake level can occur. A large lake surface area can balance bottom input mass and evaporative mass at sufficiently low water temperatures. Ultimately, a cold crater lake may form, provided that the crater wall is sufficiently high and not fragile. The most likely mechanism of an increase in crater size is coalescence with adjacent craters due to erosion of the crater walls.

At *low-*, *medium-*, and *high-activity lakes* under lake-sustainable conditions, such changes occur slowly due to the large timescales (large residence time) of these systems.

5.3.2. Conical Topography

A hot crater lake with a conical topography under lake-sustainable conditions can continue to shrink or expand due to perturbations in the water level, as shown in section 4.2. Fluctuations in precipitation are the most likely reason for perturbations in the water level. In a year when the precipitation is less than normal, the water level decreases; in such a situation, the water temperature rises, leading to a decrease in surface area because of the conical topography. Consequently, the hot crater lake can continue to shrink, accompanied by an increase in chemical concentrations, even though neither an increase in bottom input mass nor an increase in enthalpy occurs.

Indeed, we observed lake shrinkage with a corresponding rise in water temperature at Yudamari crater lake in 2011, which was not accompanied by significant increases in either SO_2 flux or seismicity (blue shading in Figure 10). Preceding the shrinkage in 2011, the water level of Yudamari was slightly above 1150 m above sea level (asl) and the crater shape was nearly cylindrical [*Terada et al*., 2008]. The bathymetry at elevations less than 1150 m is conical, meaning that lake surface area decreases with decreasing water level. We suspect that Yudamari undergoes shrinkage due to a topographic effect when the water level reaches 1150 m without any increase in subaqueous fumarolic activity, corresponding to apparent volcanic unrest.

Although shrinkage can occur without any increase in bottom input mass m_0 or enthalpy H_0, a decrease in water level may introduce mud emissions or small phreatic eruptions, similar to hydrothermal eruptions [*Browne and Lawless*, 2001], from the subaqueous fumaroles. Generally, phreatic eruptions breach a crater lake surface if the fluid pressure beneath the lake exceeds the hydrostatic pressure of the lake water. Lower lake levels could thus lead to less violent but more frequent phreatic eruptions, as pressure thresholds decrease and hence are more easily reached [*Rouwet et al*., 2014].

5.4. Implications for Long-Term Sustainability of Actual Hot Crater Lakes

On the basis of our results, we discuss the persistence of actual hot crater lakes, such as Yudamari crater lake at Aso volcano, Japan, and Yugama crater lake at Kusatsu-Shirane volcano, Japan.

5.4.1. Yudamari Crater Lake, Aso Volcano

Yudamari crater lake (*peak-activity crater lake*) lies in the first crater of Nakadake, Aso volcano, Japan, which has existed during noneruption periods for centuries [*Shinohara et al*., 2015]. Phreatomagmatic and

Strombolian eruptions have repeatedly occurred at the first crater over the past 1500 years [*Miyabuchi*, 2009; *Ono et al*., 1995]. Despite these explosive eruptions, the lake has always reformed when the volcano returns to quiescence.

The present results provide clues about why Yudamari crater lake has persisted for such a long time. We consider that stable emissions of volcanic fluid from the crater bottom have continued throughout the period of volcanic quiescence, which is appropriate for the given topography. When the first crater was smaller, water temperature was higher than at present, resulting in enhanced evaporation; hence, the lake would have shrunk, even when a crater lake is temporarily formed by intense precipitation inflow. Consequently, Yudamari would not be maintained in the long term. Conversely, if the first crater was larger than its present size, an increase in lake level would result in the formation of a large, colder crater lake with outlet streams, provided that the crater wall had sufficient height and strength.

The rate of heat discharge from Yudamari crater lake is estimated to exceed 200 MW [*Terada et al*., 2008]. The fact that Yudamari has existed for $>$1500 years suggests that the stable discharge of $>$200 MW of heat from the underlying magma at Aso volcano has also persisted for $>$1500 years, throughout a period without any major eruptions, as long as precipitation input does not change significantly on long timescales.

At altitudes less than 1150 m, the lake surface area shows marked changes with changing water levels. If water level decreases below 1150 m, Yudamari crater lake shrinks without an increase in fluid injection rate, as discussed in section 5.3.2. Consequently, there are two causes of shrinkage of Yudamari when it falls into the *peak-activity* category: an increase in mass m_0 or enthalpy H_0 of the fluid injected from the lake bottom and apparent unrest due to insufficient precipitation when water level restricts the lake to a conical bathymetry ($<$1150 m asl).

5.4.2. Yugama Crater Lake, Kusatsu-Shirane Volcano

Yugama crater lake (*high-activity crater lake*) at Kusatsu-Shirane volcano is a hot crater lake whose temperature is 10−15°C higher than the ambient air temperature [*Ohba et al*., 2008]. While Yugama has experienced concomitantly short-term disappearances of the lake due to eruptions, the lake size has grown since 1882. Prior to that year, the lake water of Yugama was acidic, although its temperature was similar to the ambient air temperature (*low activity*). Lake water occupied only a small part of the northern region of the crater; most of the crater bottom was covered by vegetation [*Ohashi*, 1914]. In 1938, a lake size of 120 × 200 m was recorded on topographical maps compiled by the Geological Survey of Japan. By 1950, the lake had grown in area to 160 × 260 m [*Minami et al*., 1952]. The present size is around 270 × 350 m [*Ohba et al*., 2008], which has been roughly constant throughout the last 30 years (Figure 11).

Recent volcanic activity at Kusatsu-Shirane includes frequent phreatic eruptions that began in 1882 [*Tsuya*, 1933; *Minakami et al*., 1943; *Ossaka et al*., 1980; *Ossaka et al*., 1997], probably caused by enhanced heating of the hydrothermal system beneath Yugama crater lake, due to magma degassing at depth.

We believe that enthalpy and mass flux of fluid injection at Yugama crater lake increased after the 1882 eruption. As a result, the status of the Yugama crater lake shifted from *low activity* to the region of an increase in water level in Figure 9. Hence, expansion of Yugama was caused by excess bottom input mass relative to evaporation loss from the lake surface, because the rise in water temperature was insufficient. The size of the lake continued to increase with stable emissions from subaqueous fumaroles because the geometry of Yugama crater around the lake bottom is conical [*Ohba et al*., 1994].

The long-term increase in lake size is probably due to the large timescales associated with the conditions of smaller m_0/S_0. Expansion of Yugama crater lake has not been observed in the last 30 years, which implies that the lake size has attained an appropriate value for long-term persistence (*high activity*) given its conditions (i.e., bottom input mass flux, enthalpy, seepage output, and precipitation input).

6. Conclusions

We investigated the conditions required for the long-term persistence of a hot crater lake. In our model, water level and temperature are controlled mainly by the enthalpy of the fluid injection H_0 and the ratio of the flux of bottom input mass to lake surface area, m_0/S_0. Given appropriate parameters (represented here by m_0/S_0 and H_0), mass and energy equilibria in the lake system are simultaneously achieved under conditions that include seepage output and precipitation input. In such cases, crater lakes can persist, even if the lake

temperature exceeds 45−50°C [*Pasternack and Varekamp*, 1997]. This result suggests that neither a high precipitation rate nor an impermeable layer beneath a lake bottom is always necessary for the long-term persistence of hot crater lakes, as long as the values of m_0 and H_0 are appropriate for the crater topography. Impermeable layer does not appear to be a requirement to form persistent hot crater lakes.

We propose that two types of hot crater lake can appear. Our results aid in interpreting changes in volcanic activity based on monitoring crater lakes. For a lake with smaller m_0/S_0, smaller H_0, and a lower water temperature, m_0 is balanced by minor evaporation mass. In such a case, water level and temperature rise with increases in m_0 and H_0, which corresponds to enhanced subaqueous fumarolic activity. In contrast to low-temperature crater lakes, high-temperature crater lakes are maintained under conditions of larger m_0/S_0 and H_0 because the larger m_0 is balanced by enhanced evaporation loss due to the higher water temperature. In such a situation, increases in m_0 and H_0 cause a decrease in the water level, accompanied by a rise in temperature. Consequently, increases or decreases in water level can occur before eruptions, depending on the values of m_0/S_0 and H_0.

Furthermore, our model shows that crater geometry is a key control on its behavior. If the lake surface area shows a marked change with changing water level, as is the case for a conical crater, then the conditions of mass and energy balance vary with changing lake level. Hence, in the case of decreasing water levels in a lake with conical topography, evaporative mass is enhanced by increasing temperature, resulting in shrinkage of the hot crater lake even when subaqueous fumarolic activity does not change. Such a shrinkage of hot crater lakes resembles the volcanic unrest that precedes eruptions.

Modifying lake bathymetry strongly influences lake-sustainable conditions. When a crater under lake-sustainable conditions shrinks (which may be caused by landslides), temperature increases and lake level decreases due to enhanced evaporation. Consequently, the hot crater lake is no longer maintained unless the fluid injection rate also changes, referred to as "apparent volcanic unrest".

Applying the present model to real examples of hot crater lakes, such as Yudamari crater lake at Aso volcano and Yugama crater lake at Kusatsu-Shirane volcano, we can interpret changes in their systems in the context of unrest. We conclude that increases in m_0/S_0 and H_0 cause a decrease in the water level of Yudamari lake and an increase in the water level of Yugama lake. We believe that the shrinkage of Yudamari crater lake in 2011 is an example of apparent unrest rather than being driven by a change in subaqueous fumarolic activity.

Appendix A: Expressions for Heat Flux Terms

Here we refer to *Terada et al*. [2012]. The total heat flux from the lake surface, Φ, can be expressed as the sum of evaporation, φ_e; conduction, φ_c; and net radiation, φ_r:

$$\Phi = \phi_e + \phi_c + \phi_r. \tag{A1}$$

Evaporation is driven by free convection due to differences between air and water temperatures and by forced convection due to horizontal wind. Hence, the evaporation heat flux depends on meteorological conditions, such as vapor pressure e_s, virtual temperature T_{vs}, and the wind speed u of the ambient air. *Ryan et al*. [1974] formulated the total evaporation heat flux φ_e as follows:

$$\phi_e = \lambda_0 (T_{vs} - T_{va})^{\frac{1}{3}} (e_s - e_a) + b_0 u (e_s - e_a), \tag{A2}$$

where e_s is vapor pressure at the water surface, corresponding to the saturation vapor pressure of water at temperature T; T_{vs} is virtual temperature in K at the water surface; and λ_0 and b_0 are empirical constants that take values of 0.027 W m^{-2} Pa^{-1} K$^{-1/3}$ and 0.032 W m^{-2} Pa^{-1} (m/s)$^{-1}$, respectively.

The saturation vapor pressure e_{sat} at temperature T is obtained from the Clausius-Clapeyron equation:

$$e_{\mathrm{sat}} = 611 \exp\left[\frac{L}{R_v}\left(\frac{1}{273.15} - \frac{1}{T + 273.15}\right)\right], \tag{A3}$$

where L is the latent heat at 273.15 K and R_v is the gas constant of vapor, 461 J kg^{-1} K^{-1}. The virtual temperature T_v at temperature T is given by

$$T_v = (T + 273.15)\left(1 + \frac{w}{0.622}\right)(1 + w)^{-1}. \tag{A4}$$

The mixing rate w is given by

$$w = \frac{0.622e}{P_a - e}, \tag{A5}$$

where e is vapor pressure and P_a is ambient air pressure.

Conduction heat loss φ_c is related to evaporation flux by Bowen's ratio [*Bowen*, 1926]:

$$\phi_c = B_o \phi_e, \tag{A6}$$

with the parameter B_o given by

$$B_o = C\frac{T_s - T_a}{e_s - e_a}, \tag{A7}$$

where $C = 61$ Pa K^{-1} is a constant.

Following *Linacre* [1992], the net radiation φ_r is given by

$$\phi_r = R_{\text{sun}} + R_{\text{rad atm}} - R_{\text{rad lake}}, \tag{A8}$$

where R_{sun} is short-wavelength solar radiation (assumed to be 100 W m^{-2}), $R_{\text{rad lake}}$ is long-wavelength radiation from the lake surface, and $R_{\text{rad atm}}$ is long-wavelength radiation from the atmosphere, given by

$$R_{\text{rad atm}} = (208 + 6T_a)\left(1 + 0.0034C_l^2\right) \tag{A9}$$

$$R_{\text{rad lake}} = \varepsilon\sigma(T_s + 273.15)^4, \tag{A10}$$

respectively. In the above equations, $\varepsilon = 0.97$ is the water surface emissivity, $\sigma = 5.67 \times 10^{-8}$ (W m^{-2} K^{-4}) is the Stefan-Boltzmann constant, l is latitude, and C_l is the average cloud cover in octos, calculated from

$$C_l = 5.1946 - 0.23227l + 6.7727\times10^{-3}l^2 - 4.9495\times10^{-5}l^3. \tag{A11}$$

Acknowledgments
We thank Takeshi Ohba, Tsuneomi Kagiyama, Yasuaki Sudo, Yasuo Miyabuchi, Takahiro Ohkura, and Shin Yoshikawa for discussions. We also thank the staff at Volcanic Fluid Research Center, Tokyo Institute of Technology, for valuable comments. We are grateful to the staff at the Japan Meteorological Agency for providing data and granting permission to use the data in this publication. We appreciate the helpful suggestions and constructive comments of Dmitri Rouwet and Jean Vandemeulebrouck, whose careful reviews have improved this manuscript. The data showing in Figure 10 are available upon request to the Japan Meteorological Agency (http://www.jma.go.jp/jma/indexe.html). We used Generic Mapping Tools [*Wessel and Smith*, 1998] to generate the figures. This work was supported by the Japanese Ministry of Education, Culture, Sorts, Science and Technology under grant 15 K01247 to A.T.

References

Agusto, M. R., A. Caselli, R. Daga, J. Varekamp, A. Trinelli, M. D. S. Afonso, M. L. Velez, P. Euillades, and S. R. Guevara (2016), The crater lake of Copahue volcano (Argentina): Geochemical and thermal changes between 1995 and 2015, *Geol. Soc. London Spec. Publ.*, *437*, 107–130, doi:10.1144/SP437.16.

Barberi, F., A. Bertagnini, P. Landi, and C. Principe (1992), A review on phreatic eruptions and their precursors, *J. Volcanol. Geotherm. Res.*, *52*(4), 231–246, doi:10.1016/0377-0273(92)90046-G.

Bowen, I. S. (1926), The ratio of heat losses by conduction and evaporation from any water surface, *Phys. Rev.*, *27*, 779–787, doi:10.1103/PhysRev.27.779.

Brantley, S. L., A. M. Agustsdottir, and G. L. Rowe (1993), Volcanic lakes reveal volcanic heat and volatile fluxes, *GSA Today*, *3*(7), 173–178.

Browne, P. R. L., and J. V. Lawless (2001), Characteristics of hydrothermal eruptions, with examples from New Zealand and elsewhere, *Earth Sci. Rev.*, *52*(4), 299–331, doi:10.1016/S0012-8252(00)00030-1.

Brown, H., H. Rymer, J. Dowden, P. Kapadia, D. Stevenson, J. Barquero, and L. D. Morales (1989), Energy budget analysis for crater lakes: Implication for predicting volcanic activity, *Nature*, *339*, 370–373, doi:10.1038/339370a0.

Christenson, B. W. (1994), Convection and stratification in Ruapehu crater Lake, New Zealand: Implications for Lake Nyos-type gas release eruptions, *Geochem. J.*, *28*, 185–197, doi:10.2343/geochemj.28.185.

Christenson, B. W. (2000), Geochemistry of fluids associated with the 1995–1996 eruption of Mt. Ruapehu, New Zealand: Signatures and processes in the magmatic-hydrothermal system, *J. Volcanol. Geotherm. Res.*, *97*, 1–30, doi:10.1016/S0377-0273(99)00167-5.

Christenson, B. W., C. A. Werner, A. G. Reyes, S. Sherburn, B. J. Scott, C. Miller, M. J. Rosenburg, A. W. Hurst, and K. A. Britten (2007), Hazards from hydrothermally sealed volcanic conduits, *Eos*, *88*(5), 53–55, doi:10.1029/2007EO050002.

Cronin, S. J., V. E. Neall, J. A. Lecointre, and A. S. Palmer (1997), Changes in Whangaehu river lahar characteristics during the 1995 eruption sequence, Ruapehu volcano, New Zealand, *J. Volcanol. Geotherm. Res.*, *76*, 47–61, doi:10.1016/S0377-0273(96)00064-9.

Fournier, N., F. Witham, M. Moreau-Fournier, and L. Bardou (2009), Boiling lake of Dominica, West Indies: High-temperature volcanic crater lake dynamics, *J. Geophys. Res.*, *114*, B02203, doi:10.1029/2008JB005773.

Fukuoka Regional Headquarters, Japan Meteorological Agency (2016), Volcanic activity of Asosan volcano -October 2014–February 2015- [in Japanese], *Reports of Coordinating Committee for Prediction of Volcanic Eruption*, pp. 166–186. [Available at http://www.data.jma.go.jp/svd/vois/data/tokyo/STOCK/kaisetsu/CCPVE/Report/120/kaiho_120_23.pdf.]

Giggenbach, W. F., and R. B. Glover (1975), The use of chemical indicators in the surveillance of volcanic activity affecting the crater lake on Mt Ruapehu, New Zealand, *Bull. Volcanol.*, *39*(1), 70–81, doi:10.1007/BF02596947.

Healy, J., E. F. Lloyd, C. J. Banwell, and R. D. Adams (1965), Volcanic eruption on Raoul Island November 1964, *Nature*, *205*, 743–745, doi:10.1038/205743a0.

Hurst, A. W., H. M. Bibby, B. J. Scott, and M. J. J. McGuinness (1991), The heat source of Ruapehu crater lake; deductions from the energy and mass balances, *J. Volcanol. Geotherm. Res.*, *46*, 1–20, doi:10.1016/0377-0273(91)90072-8.

Kanda, W., Y. Tanaka, M. Utsugi, S. Takakura, T. Hashimoto, and H. Inoue (2008), A preparation zone for volcanic explosions beneath Nakadake crater, Aso volcano as inferred from electrical resistivity surveys, *J. Volcanol. Geotherm. Res.*, *178*(1), 32–45, doi:10.1016/j.jvolgeores.2008.01.022.

Kempter, K. A., and G. L. Rowe (2000), Leakage of active crater lake brine through the north flank at Rincon de la Vieja volcano, northwest Costa Rica, and implications for crater collapse, *J. Volcanol. Geotherm. Res.*, *97*, 143–159, doi:10.1016/S0377-0273(99)00181-X.

Lecointre, J., K. Hodgson, V. Neall, and S. Cronin (2004), Lahar-triggering mechanisms and hazard at Ruapehu volcano, New Zealand, *Nat. Hazards*, *31*(1), 85–109, doi:10.1023/B:NHAZ.0000020256.16645.eb.

Linacre, E. (1992), *Climate Data and Resources. A Reference and Guide*, Routledge, Boca Raton, Fla.

Martinez, M., E. Fernandez, J. Valdes, V. Barboza, R. Van der Laat, E. Duarte, E. Malavassi, L. Sandoval, J. Barquero, and T. Marino (2000), Chemical evolution and volcanic activity of the active crater lake of Poás volcano, Costa Rica, 1993–1997, *J. Volcanol. Geotherm. Res.*, *97*, 127–141, doi:10.1016/S0377-0273(99)00165-1.

Mastin, L. G., and J. B. Witter (2000), The hazards of eruptions through lakes and seawater, *J. Volcanol. Geotherm. Res.*, *97*, 195–214, doi:10.1016/S0377-0273(99)00174-2.

Minakami, T., K. Matsuita, and S. Utibori (1943), Explosive activities of volcano Kusatu-Sirane during 1938 and 1942. (Part II), *Bull. Earthquake Res. Inst.*, *20*, 505–534.

Minami, E., N. Yamagata, M. Shima, and Y. Saijo (1952), Crater Lake "Yugama" of Volcano Kusatsu-Shirane. I. [in Japanese], *Jpn. J. Limnol.*, *16*, 1–5.

Miyabuchi, Y. (2009), A 90,000-year tephrostratigraphic frame work of Aso Volcano, Japan, *Sediment. Geol.*, *220*, 169–189, doi:10.1016/j.sedgeo.2009.04.018.

Miyabuchi, Y., and A. Terada (2009), Subaqueous geothermal activity revealed by lacustrine sediments of the acidic Nakadake crater lake, Aso Volcano, Japan, *J. Volcanol. Geotherm. Res.*, *187*, 140–145, doi:10.1016/j.jvolgeores.2009.08.001.

Miyabuchi, Y., S. Ikebe, and K. Watanabe (2008), Geological constraints on the 2003-2005 ash emissions from the Nakadake crater lake, Aso Volcano, Japan, *J. Volcanol. Geotherm. Res*, *178*(2), 169–183, doi:10.1016/j.jvolgeores.2008.06.025.

Morrissey, M., G. Gisler, R. Weaver, and M. Gittings (2010), Numerical model of crater lake eruptions, *Bull. Volcanol.*, *72*(10), 1169–1178, doi:10.1007/s00445-010-0392-5.

Ohba, T., J. Hirabayashi, and K. Nogami (1994), Water, heat and chloride budgets of the crater lake Yugama at Kusatsu-Shirane Volcano, Japan, *Geochem. J.*, *28*(3), 217–231, doi:10.2343/geochemj.28.217.

Ohba, T., J. Hirabayashi, and K. Nogami (2008), Temporal changes in the chemistry of lake water within Yugama Crater, Kusatsu-Shirane Volcano, Japan: Implications for the evolution of the magmatic hydrothermal system, *J. Volcanol. Geotherm. Res.*, *178*(2), 131–144, doi:10.1016/j.jvolgeores.2008.06.015.

Ohashi, Y. (1914), The volcano Shirane, Prov. Kotsuke (IV) [in Japanese], *J. Geol. Soc. Tokyo*, *21*, 359–368.

Ono, K., K. Watanabe, H. Hoshizumi, and S. Ikebe (1995), Ash eruption of Nakadake crater, Aso volcano, southwestern Japan, *J. Volcanol. Geotherm. Res.*, *66*, 137–148, doi:10.1016/0377-0273(94)00061-K.

Ossaka, J., T. Ozawa, T. Nomura, T. Ossaka, J. Hirabayashi, A. Takaesu, and T. Hayashi (1980), Variation of chemical compositions in volcanic gases and waters at Kusatsu-Shirane volcano and its activity in 1976, *Bull. Volcanol.*, *43*(1), 207–216, doi:10.1007/BF02597622.

Ossaka, J., T. Ossaka, J. Hirabayashi, T. Oi, T. Ohba, K. Nogami, Y. Kikawada, M. Yamano, M. Yui, and H. Fukuhara (1997), Volcanic activity of Kusatsu-Shirane volcano, Gunma, and secular change in water quality of crater lake Yugama [in Japanese with English abstract], *Geochemistry*, *31*, 119–128, doi:10.14934/chikyukagaku.31.119.

Pasternack, G. B., and J. C. Varekamp (1997), Volcanic lake systematics I. Physical constraints, *Bull. Volcanol.*, *58*(7), 528–538, doi:10.1007/s004450050160.

Rouwet, D. (2011), A photographic method for detailing the morphology of the floor of a dynamic crater lake: The El Chicho'n case (Chiapas, Mexico), *Limnology*, *12*(3), 225–233, doi:10.1007/s10201-011-0343-7.

Rouwet, D., and F. Tassi (2011), Geochemical monitoring of volcanic lakes. A generalized box model for active crater lakes, *Ann. Geophys.*, *54*, 161–173, doi:10.4401/ag-5035.

Rouwet, D., Y. A. Taran, and N. R. Varley (2004), Dynamics and mass balance of El Chicho'n crater lake, Mexico, *Geofis. Int.*, *43*, 427–434.

Rouwet, D., F. Tassi, R. Mora-Amador, L. Sandri, and V. Chiarini (2014), Past, present and future of volcanic lake monitoring, *J. Volcanol. Geotherm. Res.*, *272*, 78–97, doi:10.1016/j.jvolgeores.2013.12.009.

Rouwet, D., R. Mora-Amador, C. J. Ramírez-Umaña, G. González, and S. Inguaggiato (2016), Dynamic fluid recycling at Laguna Caliente (Poas, Costa Rica) before and during the 2006-ongoing phreatic eruption cycle (2005-10), *Geol. Soc. London Spec. Publ.*, *437*, 73–96, doi:10.1144/SP437.11.

Rowe, G. L., S. L. Brantley, M. Fernandez, J. F. Fernandez, A. Borgia, and J. Barquero (1992), Fluid-volcano interaction in an active stratovolcano; the crater lake system of Poás Volcano, Costa Rica, *J. Volcanol. Geotherm. Res.*, *49*, 23–51, doi:10.1016/0377-0273(92)90003-V.

Ryan, P. J., D. R. Harleman, and K. D. Stolzenb (1974), Surface heat loss from cooling ponds, *Water Resour. Res.*, *10*(5), 930–938, doi:10.1029/WR010i005p00930.

Schaefer, J. R., W. E. Scott, W. C. Evans, J. Jorgenson, R. G. McGimsey, and B. Wang (2008), The 2005 catastrophic acid lake drainage, lahar, and acidic aerosol formation at Mount Chiginagak volcano, Alaska, USA: Field observations and preliminary water and vegetation, hemistry results, *Geochem. Geophys. Geosyst.*, *9*(7), Q07018, doi:10.1029/2007GC001900.

Shinohara, H., S. Yoshikawa, and Y. Miyabuchi (2015), Degassing Activity of a Volcanic Crater Lake: Volcanic Plume Measurements at the Yudamari Crater Lake, Aso, in *Volcanic Lakes*, edited by D. Rouwet et al., pp. 201–217, Springer-Heidelberg, doi:10.1007/978-3-642-36833-2_8.

Simkin, T., and L. Siebert (1994) *Volcanoes of the World*, Second ed., p. 349, Geoscience Press, Inc., Tucson, Arizona, ISBN 0-945005-12-1

Takano, B., K. Suzuki, K. Sugimori, T. Ohba, S. M. Fazlullin, A. Bernard, S. Sumarti, R. Sukhyar, R. Sukhya, and M. Hirabayashi (2004), Bathymetric and geochemical investigation of Kawah Ijen crater lake, east Java, Indonesia, *J. Volcanol. Geotherm. Res.*, *135*(4), 299–329, doi:10.1016/j.jvolgeores.2004.03.008.

Takano, B., and K. Watanuki (1990), Monitoring of volcanic eruptions at Yugama crater lake by aqueous sulfur oxyanions, *J. Volcanol. Geotherm. Res.*, *40*(1), 71–87, doi:10.1016/0377-0273(90)90107-Q.

Tamburello, G., et al. (2015), Intense magmatic degassing through the lake of Copahue volcano, 2013-2014, *J. Geophys. Res. Solid Earth*, *120*, 6071–6084, doi:10.1002/2015JB012160.

Taran, Y., and D. Rouwet (2008), Estimating thermal inflow to El Chichón crater lake using the energy-budget, chemical and isotope balance approaches, *J. Volcanol. Geotherm. Res.*, *175*(4), 472–481, doi:10.1016/j.jvolgeores.2008.02.019.

Tassi, F., O. Vaselli, B. Capaccioni, C. Giolito, E. Duarte, E. Fernandez, A. Minissale, and G. Magro (2005), The hydrothermal-volcanic system of Rincon de la Vieja volcano (Costa Rica): A combined (inorganic and organic) geochemical approach to understanding the origin of the fluid discharges and its possible application to volcanic surveillance, *J. Volcanol. Geotherm. Res.*, *148*, 315–333, doi:10.1016/j.jvolgeores.2005.05.001.

Tassi, F., O. Vaselli, E. Fernández, E. Duarte, M. Martínez, A. Delgado-Huertas, and F. Bergamaschi (2009), Morphological and geochemical features of crater lakes in Costa Rica: An overview, *J. Limnol.*, *68*(2), 193–205, doi:10.3274/JL09-68-2-04.

Terada, A., T. Hashimoto, T. Kagiyama, and H. Sasaki (2008), Precise remote-monitoring technique of water volume and temperature of a crater lake in Aso volcano, Japan: Implication for a sensitive window of volcanic hydrothermal system, *Earth Planets Space*, *60*(6), 705–710, doi:10.1186/BF03353134.

Terada, A., T. Hashimoto, and T. Kagiyama (2012), Volcanic lake system at Aso volcano, Japan: Fluctuations in the supply of volcanic fluid from the hydrothermal system beneath the crater lake, *Bull. Volcanol.*, *74*(3), 641–655, doi:10.1007/s00445-011-0550-4.

Todesco, M., D. Rouwet, M. Nespoli, and M. Bonafede (2015), How steep is my seep? Seepage in volcanic lakes, hints from numerical simulations, in *Volcanic Lakes*, edited by D. Rouwet et al., pp. 323–339, Springer-Heidelberg, Heidelberg, doi:10.1007/978-3-642-36833-2_14.

Tokyo Institute of Technology, and Sophia University (1984), Geochemical study of volcanic activity of Kusatsu-Shirane volcano in 1982–1983 (3) [In Japanese], *Reports of Coordinating Committee for Prediction of Volcanic Eruption*, vol. 30, pp. 64–73.

Tsuya, H. (1933), Explosive activity of volcano Kusatu-Sirane in October, 1932, *Bull. Earthquake Res. Inst.*, *11*, 82–112.

Vandemeulebrouck, J., J. C. Sabroux, M. Halbwachs, Surono, N. Poussielgue, J. Grangeon, and J. Tabbagh (2000), Hydroacoustic noise precursors of the 1990 eruption of Kelut Volcano, Indonesia, *J. Volcanol. Geotherm. Res.*, *97*, 443–456, doi:10.1016/S0377-0273(99)00176-6.

Vandemeulebrouck, J., D. Stemmelen, T. Hurst, and J. Grangeon (2005), Analogue modeling of instabilities in crater lake hydrothermal systems, *J. Geophys. Res.*, *110*, B02212, doi:10.1029/2003JB002794.

Varekamp, J., A. Ouimette, S. Herman, A. Bermudez, and D. Delpino (2001), Hydrothermal element fluxes from Copahue, Argentina: A "beehive" volcano in turmoil, *Geology*, *29*(11), 1059–1062, doi:10.1130/0091-7613(2001)029<1059:HEFFCA>2.0.CO;2.

Wessel, P., and W. H. F. Smith (1998), New, improved version of generic mapping tools released, *Eos Trans. AGU*, *79*(47), 579, doi:10.1029/98EO00426.